4

INTERSPECIES COMPARISONS IN THE UNDERSTANDING OF HUMAN VISUAL PERCEPTION

M. L. J. Crawford, Richard A. Andersen, Randolph Blake, Gerald H. Jacobs, and Christa Neumeyer

I. INTRODUCTION

A. Why Study Other Species?

The history of the advance of knowledge in the biological sciences is replete with examples of how the study of other species has been indispensable to scientific progress. No area of biology would have developed to any significant degree without the contributions made by observations and research carried out on animals. Since the time of Galen, the study of the anatomical and physiological systems in animals has established the foundation for inferences drawn concerning possible physiological substrates for human perception, and has provided, as well, the basis for speculation about mechanisms underlying behavioral and perceptual processes in the species itself.

This information transfer has not always been unidirectional, that is, from animal physiology to human perception. It has also worked the other way around. The study of human perception through visual psychophysics has often guided the study of anatomy and physiology in animals. For example, consider stereopsis, the appreciation of depth from binocular viewing (see Chapter 12, this volume). The perceptual aspects of stereopsis have been recognized since Aristotle and have received sporadic attention throughout history. In the last century, Wheatstone (1838) demonstrated that horizontal disparity of the binocular images was sufficient to produce the perception of depth, and Herman Wilbrand speculated rather accurately about the anatomical substrate of stereopsis at least 60 years before it was actually demonstrated. Wilbrand concluded that the two homononymous hemiretinas were represented in the same overlapping area of the cortex, and that retinal point-pairs, from the left and right eye, interacted to provide the basis for stereopsis (Polyak, 1957). Through continuing psychophysical study (e.g., Ogle, 1950; Julesz, 1960) the requirements of the neural substrates for stereopsis became increasingly evident. The actual demonstration came from the experiments of Barlow, Blakemore, and Pettigrew (1967) and Pettigrew, Nikara,

and Bishop (1968) in their electrophysiological studies of cat cortex. Since then, the work of Bishop (see Bishop & Pettigrew, 1986), Poggio (see Chapter 12, this volume), and Crawford (Crawford et al., 1983, Crawford, Smith, Harwerth & von Noorden, 1984) leaves little doubt that cortical binocular cells provide the physiological basis for stereopsis.

From this example it can be seen that the study of other species serves at least four valuable purposes: (1) to determine the anatomical and physiological *substrate* of perceptual processes; (2) to gain better *experimental control* over the subject of study, for example, being able to manipulate the kind and degree of visual experience during visual development; (3) to work out the *rules* for how anatomical, physiological, developmental, and behavioral variables determine the function of a sensory or perceptual system; and (4) to test the *generality* of these rules across species. The closer the species, phylogenetically, the more likely the solutions to the problem have common elements between the species.

B. What Makes a Good Animal Model for Human Visual Perception?

Ideally one would want an animal research model for visual perception to have the same anatomical, physiological, and behavioral attributes as that of humans. Of course, practical animal models may approximate only one or more characteristics of the human visual system. Bearing in mind that, in the absence of language, it is virtually impossible to equate perceptual phenomena between human and animal observers, sensory parameters can be explored in both humans and other animals, often using the same measurement apparatus and procedures. Some of the more obvious desirable and practical characteristics of an animal model are as follows:

1. The species should exhibit the visual behavior of interest in its natural environment.
2. The species should possess anatomical characteristics which permit extrapolation to comparable structures in humans.
3. The species should demonstrate discriminative behaviors suggestive of comparable processes in humans (e.g., color-matching, hue discrimination, stereopsis, visual development).
4. The species should be an "appropriate" experimental subject according to the following criteria:
   a. Predictability: The animal should give a consistent behavioral response, that is, a low variance of response.
   b. Availability: The animal should be available in sufficient numbers, and at an affordable cost, so as to permit replication of experimental research.
   c. Convenience: The animal should be of a size and disposition conducive to handling.
   d. Ethical considerations: The animal should merit use as a research model. Sacrifice of rare or endangered species should not be acceptable.

The following sections are intended to illustrate these considerations in selecting the particular species of animal subject, and in the interpretations and generalizations of results to processes in other species and to perceptual processes in humans. The reader is urged to refer to the logical constraints described in Chapter 3 of this volume in order to better interpret the conclusions drawn about the relations between brain function in experimental animals and human visual perception.

II. COMPARATIVE ASPECTS OF CAT SPATIAL VISION

Let us begin with a description of the comparative vision of the cat, visual science's most popular nonhuman research species. The cat has contributed enormously to our understanding of the neuroanatomy and neurophysiology of mammalian vision. Indeed, many of the hallmark properties of mammalian visual neurophysiology were discovered and elaborated in the cat. These include the center–surround organization of retinal ganglion cell receptive fields (Kuffler, 1953),

the existence of multiple parallel visual pathways (i.e., *X*, *Y*, and *W* pathways) from retina to brain (Enroth-Cugell & Robson, 1966), and the orientation selectivity and binocularity of cortical cells (Hubel & Wiesel, 1962).

This wealth of neurophysiological and neuroanatomical data about the cat's visual system raises two questions: (1) To what extent can the visual capacities of the cat be explained in terms of the sampling constraints and receptive field properties of retinal, geniculate, and cortical neurons? (2) To what extent are cat and human visual performance comparable? The first question, of course, addresses one of the most fundamental issues of sensory neuroscience, the neural basis of perception. The second question relates directly to the first one; to the extent that human and cat vision are comparable, one may reasonably assume that neurophysiological findings in the cat shed light on the neural machinery of human vision. In this section we review evidence that bears on these two questions, with particular emphasis on spatial vision (i.e., the detection and discrimination of objects and displays defined by luminance contours). It is useful to start with a few general comments concerning strategies for comparing psychophysical data with physiological data.

A. Physiology and Psychophysics

In evaluating the relation between cat physiology and cat psychophysics, we shall want to compare measures of neural responsiveness (e.g., firing rate) with measures of behavioral performance (e.g., contrast detection threshold). What conditions must be satisfied for this comparison to be meaningful? To begin, the same stimulus should be employed in both types of measurements. For instance, to learn about contrast coding, we might employ a sinusoidal grating to generate action potentials (the physiological measure) as well as to measure contrast thresholds (the psychophysical measure); it would make little sense to compare neural data collected with spots of light to behavioral data obtained using a grating.

Simply employing the same physical stimulus, however, does not ensure equivalence between the two types of experiments. In physiological experiments, the animal's eyes may be dilated and/or immobilized, whereas in a behavioral experiment natural pupils and freely moving eyes are the rule. Hence, retinal illuminance (determined by pupil size) and temporal frequency (influenced by eye movements) may differ significantly in the two types of experiments; this means that a given physical stimulus may not be truly equivalent in the two experiments. This lack of stimulus equivalence can be minimized by recording from an alert, behaving animal, but this requires training the animal to maintain fixation so that the visual stimulus can be accurately placed in the receptive field of the neuron whose activity is being recorded. An alternative solution is to coordinate the design of stimuli in psychophysical and physiological experiments so that equivalent optical quality, retinal illuminance, etc. are ensured. Still, certain factors will be very difficult to equate.

Next comes the problem of data comparison. How does one compare the responsiveness of a neuron or class of neurons with an animal's performance on a threshold task? Even with the same stimulus providing a common denominator, how can one relate a neuronal response to a given stimulus to a behavioral response elicited by that same stimulus? One strategy might involve measuring the minimum stimulus value that elicits a reliable response, perhaps employing some type of signal detection task to define a physiological threshold (e.g., Bradley, Skottun, Ohzawa, Sclar & Freeman, 1987). However, to the extent that different cells exhibit different thresholds, one must posit some decision rule specifying how signals from these different cells contribute to a psychophysical judgment. Are such judgments based on activity within the most sensitive neuron, on some weighted average of neural activity, or what? And, what is the particular performance level required (e.g., 75% correct) to define threshold? In view of these considerations, it is unrealistic to expect strict equivalence between a physiological threshold and a psychophysical threshold.

A second, more realistic, strategy for relating psychophysics to physiology entails deriving a family of

psychophysical thresholds and expressing these thresholds in the form of a psychophysical function. The term "psychophysical function" refers to a plot showing the variation in threshold (e.g., the dimmest light increment that elicits a response) with some stimulus dimension (e.g., wavelength). The resulting spectral sensitivity function (in this example) defines the bandwidth of the system for that stimulus dimension, and, it is hoped, the function will exhibit some characteristic shape, or signature (e.g., nonmonotonicity). Now one can compare this psychophysical function to the same sort of function defined physiologically. The two functions can be compared in terms of their shapes and bandwidths. This comparison provides a more compelling test of the equivalence hypothesis, because it involves comparing changes in threshold over some common stimulus dimension. Interestingly, for some stimulus dimensions, the bandwidth determined behaviorally greatly exceeds the bandwidths of individual neural elements. To give an example, the cat can resolve spatial frequencies spanning roughly a 5-octave range (Blake, Cool & Crawford, 1974), yet individual neurons typically respond over a much narrower range of frequencies (Movshon, Thompson & Tolhurst, 1978a). The upper and lower limits of this range vary from cell to cell, however, and the total range encompassed by a large sample of cells matches the 5-octave bandwidth measured behaviorally.

A third strategy for relating psychophysics to underlying neural processes involves generating quantitative predictions of visual performance derived from anatomy. For instance, sampling theory specifies the highest resolvable frequency that can be unambiguously registered by an array of neural elements. This so-called Nyquist limit (see Chapter 10, this volume) can be computed from density estimates for, say, retinal ganglion cells, and this limit, in turn, can be compared against behavioral performance. Similarly, one can compute Nyquist limits for two different species to predict the extent to which the two species should perform differently on a visual task.

A fourth, potentially powerful strategy is to correlate deficits in behavioral performance with disorders in the visual nervous system. These disorders could occur naturally (e.g., reduced cortical binocularity in Siamese cats) or could be experimentally induced (e.g., reduced binocularity from alternating monocular deprivation early in life). This strategy has been employed with great success (e.g., Lehmkuhle, Kratz & Sherman, 1982), in part because so much has been learned about the effects of early visual deprivation (e.g., Movshon & Van Sluyters, 1981). In effect, physiologists have devised recipes (i.e., early rearing techniques) for altering the visual nervous system in interesting and suggestive ways. Psychophysicists were quick to capitalize on these recipes to study the behavioral concomitants of these neural deprivation effects. Moreover, it has been possible to find and study humans with comparable histories of early visual deprivation, thereby forging a link between clinical ophthalmology and visual neurophysiology (e.g., Holopigian, Blake & Greenwald, 1986).

These, then, are some strategies for extrapolating from physiology to psychophysics and for generalizing from an animal species to humans. Versions of these strategies have been employed in the study of cat spatial vision, and results from those studies are the major focus of this section of the chapter. In evaluating behavioral data on cat spatial vision, it is useful to keep in mind those factors, optical and neural, that could influence the quality of cat spatial vision and its comparability to human spatial vision. Accordingly, a summary of those factors is given in the next subsection.

B. Optical and Neural Determinants of Cat Spatial Vision

The design of any visual system involves a compromise between light sensitivity and spatial resolution—those adaptations that favor one almost always detract from the other. In the case of the cat, this compromise between sensitivity and resolution leans in favor of sensitivity, at least by human standards, a compromise that makes sense given this animal's nocturnal leanings. It is useful to keep this thought in mind as

we consider the optical and neural factors that govern cat spatial vision.

1. Optics of the Cat Eye

Looking first at the optical system in the cat, the eyeball itself is relatively large, with a broad light-gathering cornea, a pupil with an enormous dynamic range, and a globular lens placed relatively far back in the eye. Assuming average values for the dioptric components of the eye (Vakkur & Bishop, 1963), one degree of visual angle subtends 0.218 mm on the retina, a value approximately 30% smaller than that estimated for the human. The retinal illuminance associated with this smaller image, however, will be brighter, by as much as 5 times under dim light conditions when the pupil is fully dilated. The total range of accommodation in the cat has been estimated to be 4 D (diopters) (Vakkur, Bishop & Kozak, 1963), and its near point falls around 25 cm (Bloom & Berkley, 1977). Interestingly, accommodation in the cat appears to be accomplished by actual movement of the principal planes of the lens (Hughes, 1973), not by an increase in lens power.

Turning next to the optical performance of the cat's eye, Robson and Enroth-Cugell (1978) have derived a modulation transfer function (MTF) for the cat's optics (i.e., a plot of the ratio of image contrast to target contrast at different spatial frequencies). When the test target was imaged through a 4 mm artificial pupil, the cutoff spatial frequency (i.e., the highest spatial frequency passed by the optics) equaled approximately 20 cycles/degree. Under natural viewing conditions, the cat would have to view a surface whose average luminance was approximately 500 cd/m^2 for its pupil to be equivalent in area to that produced by an artificial pupil 4 mm in diameter (Hammond & Mouat, 1985). While this light level is easily realizable under daylight viewing conditions, it is unusual to work at light levels as high as 500 cd/m^2 in the laboratory. This means that during most behavioral work the cat's pupil will be larger than 4 mm, and, therefore, the quality of the image on the cat's retina will be somewhat poorer because of the enlarged pupil. To illustrate, when viewing a surface luminance of 40 cd/m^2 (a value within the range typically used in behavioral work), pupil size in the cat increases to approximately 55 mm^2, which would be equivalent to viewing through a circular artificial pupil a little over 8 mm in diameter. Optical quality in the cat has not been measured with an artificial pupil so large, therefore, we can only speculate about the quality of the retinal image produced under these conditions. Robson and Enroth-Cugell (1978) did measure the line-spread function through the cat's natural pupil (size unspecified), and the cutoff frequency of the derived MTF fell around 15 cycles/degree. Thus, knowing nothing else about the cat's visual system, we can expect the optics of the cat's eye to impose a limit on the cat's acuity somewhere between 15 and 20 cycles/degree.

2. The Cat Retina

The cat, like the human, possesses a duplex retina in which rods far outnumber cones (Steinberg, Reid and Lacy, 1973). Even within the region of maximum cone density, the area centralis, rods are 10 times more numerous than cones, in marked contrast to the rod-free human fovea. The density of cones within the area centralis is about 27,000 cones/mm^2; rod density in the area centralis equals about 275,000 rods/mm^2. Recalling that 1 degree visual angle corresponds to 0.218 mm, we can express cone and rod density in angular units: a 1 degree^2 region centered on the area centralis contains approximately 1225 cones and 13,000 rods. On average, neighboring cones are separated by 1.7 arc min, while rod separation is about 0.54 arc min. The visual significance of these figures is considered when we discuss acuity. Incidentally, the degree of regularity in the spatial distribution of the mixed photoreceptor mosaic has been described by Steinberg et al. (1973) and Wässle and Riemann (1978). Both groups have noted a significant departure from strict regularity in the cone array, and Wässle and Riemann have contrasted this with the rather precise mosaic of cones in the monkey fovea.

Because the entire cat retina, including the area

centralis, contains a mixed photoreceptor population, it is important to know something about the luminance conditions at which a single photoreceptor system exclusively contributes to visual performance in the cat. Only by working above the upper luminance level for mesopic vision can visual performance be unambiguously related to sampling properties of the cat's cone mosaic, or only by working below the lower luminance level for mesopic vision will performance be exclusively rod based. Ganglion cell data and pupil area data can be used to estimate the upper and lower bounds on the mesopic range for an awake cat viewing its environment through natural pupils. Enroth-Cugell, Hertz, and Lennie (1977) used a two-color isolation procedure to measure light levels at which ganglion cells received cone input only and rod input only. Over a sample of 11 cells, the upper limit of the mesopic range varied from 2.5 to 3.5 log cd/m^2, and the lower limit varied between -0.8 and 0.2 log cd/m^2. These values were based on a pupil 1 mm^2 in diameter, so they can be interpreted as cat trolands (i.e., estimates of retinal illuminance, the product of luminance and pupil area). Taking average values from Enroth-Cugell et al. for the two extremes of the mesopic range, the curves of Hammond and Mouat (1985) were used to determine the light level that would produce these values of retinal illuminance with natural pupils. According to this analysis, cat ganglion cells should receive pure rod input when the prevailing level of luminance falls anywhere below 0.1 cd/m^2 and pure cone input whenever this level exceeds 50 cd/m^2. The mesopic range in the cat, therefore, spans slightly less than a 3 log-unit range of luminance.

Like the photoreceptors, ganglion cells reach peak density in the area centralis. All ganglion cells receive inputs from both rods and cones, although the β type ganglion cells, which are thought to correspond to the physiologically defined X cells, appear to receive a larger proportion of cone input than do the α cells, thought to be Y cells (e.g., Steinberg et al., 1973). Grouping ON and OFF cells together, β cell density in the area centralis has been estimated to be approximately 6,000/mm^2 (Hughes, 1981). This value is almost 5 times lower than the cone density in the area centralis, implying convergence of many cones onto single ganglion cells. In the primate fovea, there is evidence for 1:1 convergence of single cones onto individual ganglion cells.

3. Cortical sampling

Finally, the packing density of neurons in cat visual cortex (i.e., number of cells/cubic millimeter) is 2.5 times less than in monkey visual cortex (Beaulieu & Colonnier, 1983), and the total number of neurons in Area 17 of cat is estimated to be 6 times less than in Area 17 of the monkey. In view of these numerical disparities, it is natural to expect that the cat's cortex provides less fine-grained reconstruction of the retinal image than does the monkey or human cortex (Barlow, 1979).

C. Visual Resolution in Cats and Humans

1. Visual Acuity

Over the years, a number of laboratories have determined the cat's visual acuity; the consensus of these experiments places that figure in the neighborhood of 6–8 cycles/degree (Smith, 1936; Blake et al., 1974; Jacobson, Franklin & McDonald, 1976; Bloom & Berkley, 1977; Mitchell, Giffin & Timmey, 1977; Vandenbussche & Orban, 1983). Most of these measurements were performed, incidentally, at light levels in the upper mesopic and lower photopic range for the cat. Unlike in man, the cat's threshold acuity does not seem to vary with grating orientation (Vandenbussche & Orban, 1983), which is somewhat surprising given the preponderance of visual cortical cells tuned to the principal meridians (e.g., Rose & Blakemore, 1974). The cat's visual acuity does vary, however, with retinal eccentricity, and, as illustrated in Fig. 1, the falloff in the cat's acuity with eccentricity mirrors rather closely the falloff in human acuity. The human acuity measurements (Berkley et al., 1975) were made using a 60% contrast vertical grating that flickered at 1 Hz; the cat data (Blake & Bellhorn, 1978) were collected using a 45% contrast vertical grating flickering at 1.5 Hz.

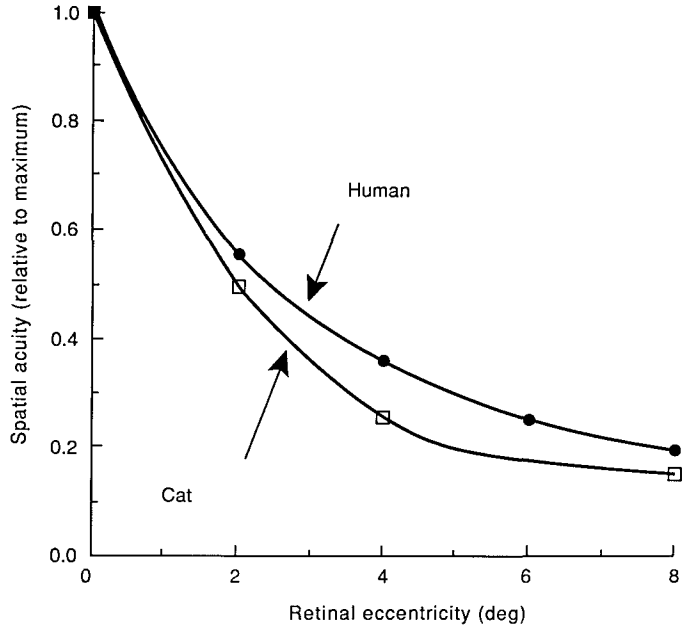

Fig. 1 The falloff in visual acuity with retinal eccentricity for the cat (Blake & Bellhorn, 1978) and human (Berkley et al., 1975). Acuity is defined as the highest resolvable spatial frequency of a grating.

What factors limit spatial resolution in the cat? It is doubtful that the cat's optics are responsible for the animal's acuity, for the high frequency cutoff of the modulation transfer function (Robson & Enroth-Cugell, 1978) is near 20 cycles/degree. Moreover, the Nyquist limit of the cone mosaic of the cat's area centralis comes to about 18 cycles/degree, and the falloff in cone density with eccentricity is more gradual than the falloff in the cat's acuity (see Fig. 2). These two observations strongly suggest that acuity is not being limited by the sampling density of the cones. The falloff in β cell density with eccentricity does, however, dovetail nicely with the progressive loss in the cat's visual acuity with retinal eccentricity, (Fig. 2). This correspondence suggests that convergence of cone signals onto ganglion cells may be a major limit to visual acuity in the cat. At present it is impossible to say whether ON and OFF systems of the β cell population act in concert, or independently, to set limits on acuity (Hughes, 1981).

How does this conclusion compare to the situation in humans? In the human eye, optics, cone sampling density, and β ganglion cell sampling density all yield

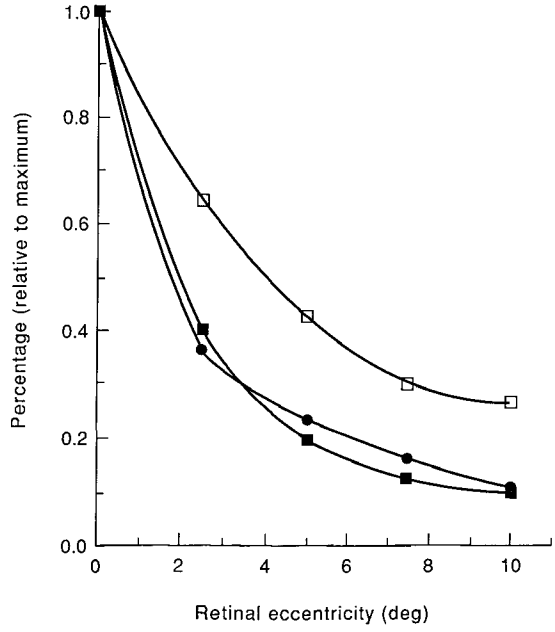

Fig. 2 Grating acuity in the cat at different retinal eccentricities compared with cone and ganglion cell density at the same locations.

approximately the same estimate of foveal acuity, 60 cycles/degree, which closely matches the value actually obtained under optimal conditions (see Chapter 10, this volume). The falloff in acuity with eccentricity, however, correlates well with the change in density of β ganglion cells and does not match the change in density of cones, suggesting that the same factor, pooling of signals by ganglion cells, limits visual resolution in cats and in humans.

How well does the cat's behaviorally measured acuity match the best resolution exhibited by single cells? In the retina, ganglion cells of the brisk-sustained type (thought to be the β type cells) with receptive fields in the area centralis can resolve gratings as high as 9 cycles/degree (Cleland, Harding & Tulunay-Keesey, 1979). Moving away from the area centralis, cutoff frequencies for this class of ganglion cells are systematically lower and, in fact, follow very closely the falloff in β cell density shown in Fig. 2. Comparable acuity values (i.e., approximately 7 cycles/degree) have been reported for X cells in the lateral geniculate nucleus (Lehmkuhle et al., 1980) and for simple cells in Area 17 (Eggers & Blakemore, 1978; Movshon, Thompson & Tolhurst, 1978b). In other visual areas, including Area 18 (Movshon et al., 1978a), the lateral suprasylvian cortex (DiStefano, Morrone & Burr, 1985; Zumbroich & Blakemore, 1987), and the superior colliculus (Bisti & Sireteanu, 1976), cells are unable to resolve spatial frequencies higher than 2.5 cycles/degree. These observations implicate Area 17 as the cortical region crucially involved in the resolution of fine spatial detail. In this regard, it is notable that lesions of Area 17 in the cat produce about a 30% reduction in grating acuity (Berkley & Sprague, 1979) and even greater losses in the ability to detect vernier offsets (Sprague, Berkley & Hughes, 1979).

2. Spatial Contrast Sensitivity

Several laboratories (Bisti & Maffei, 1974; Blake et al., 1974) have measured the cat's contrast sensitivity function (CSF), that is, the curve depicting variations in the reciprocal of contrast threshold with spatial frequency. Representative results are shown in Fig. 3, which shows CSFs measured for the cat and for a hu-

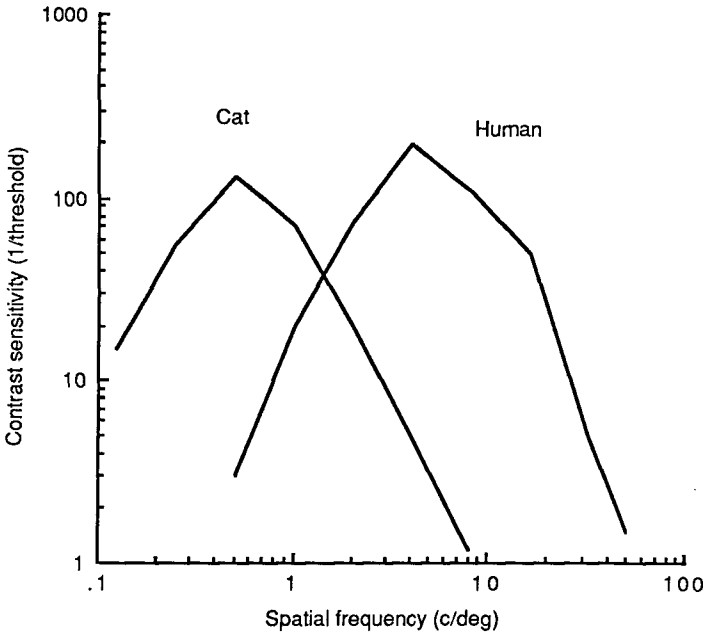

Fig. 3 Contrast sensitivity functions for the cat and human.

man under comparable stimulus conditions (i.e., stationary gratings presented at a low photopic background level). While both functions span roughly a 5-octave range of spatial frequencies, the peak of the CSF for the cat is situated about 3 octaves lower than the peak of the human CSF. Humans, in other words, see high spatial frequencies invisible to the cat, whereas the cat sees low spatial frequencies invisible to humans.

The shape of the cat's CSF varies with the rate of the temporal modulation of the bars of the grating (Blake & Camisa, 1977; Pasternak et al., 1985) as well as with background luminance level (Pasternak & Merigan, 1981). Specifically, drifting or flickering a grating impairs contrast sensitivity at higher spatial frequencies while at the same time improving sensitivity at low spatial frequencies. Lowering the background luminance level depresses sensitivity at all spatial frequencies. These same stimulus variables, luminance and temporal modulation, have an equivalent effect on the shape of the human CSF (e.g., see Robson, 1966; DeValois, Morgan, Polson, Mead & Hull, 1974).

D. The Neural Basis of Contrast Sensitivity in the Cat

Turning to the question of underlying neural mechanisms, some investigators (Blake & Camisa, 1977; Blake & DiGianfilippo, 1980; Lehmkuhle, Sherman & Kratz, 1984) have proposed that X cells are primarily responsible for the cat's contrast sensitivity at high spatial frequencies while Y cells mediate grating detection at low spatial frequencies. Several lines of evidence led to this proposal. First, it was originally thought that Y cells respond to low spatial frequencies that fail to activate X cells, while X cells respond to high spatial frequencies unresolvable by Y cells (e.g., Derrington & Fuchs, 1979; Lehmkuhle et al., 1980). More recently, however, it has been shown that Y cells do exhibit a measurable response to high spatial frequencies (So & Shapley, 1979), so one cannot be certain that resolution of high spatial frequencies is exclusively the province of X cells. Second, several laboratories have measured losses in contrast sensitivity in cats deprived of patterned binocular input during kittenhood and found those losses to be most pronounced at low spatial frequencies (Blake & DiGianfilippo, 1980; Lehmkuhle et al., 1984). This matched well with reports that binocular deprivation early in life reduces the incidence of Y cells in the lateral geniculate nucleus while leaving the number of X cells relatively unaltered (e.g., Kratz, Sherman & Kalil, 1979). Because of electrode sampling bias, however, one must interpret this finding with caution (see Shapley & So, 1980). All things considered, the hypothesis that X and Y cells differentially contribute to the cat's CSF remains largely speculative.

What is clear, however, is that the detection of grating patterns by the cat is mediated by neurons narrowly tuned for spatial frequency and orientation. This conclusion comes from masking experiments in which cats were required to detect sinusoidal gratings that appeared superimposed upon one-dimensional noise (Blake & Martens, 1981; Blake & Holopigian, 1985). The spatial frequency content and the orientation of the noise were varied relative to the frequency and orientation of the test grating, to determine the extent to which the noise impaired detection of the grating. The resulting masked thresholds were plotted in the form of "tuning curves," and some typical results are shown in Fig. 4.

Looking first at the pair of curves in the top panel, notice that noise impaired grating detection only when the spatial frequencies in that noise were within about 2 octaves of the test spatial frequency; noise further removed from the test frequency had no influence on detection, although that noise remained highly visible. The behavioral tuning curves derived from masking were also consistently broader and somewhat asymmetric for the lower test spatial frequency. These tuning width estimates and the somewhat broader, asymmetric tuning at lower frequencies are characteristic of spatial tuning curves for neurons in Area 17 of the cat's cortex. In contrast, cortical cells in Area 18 (Movshon et al., 1978b) and in the lateral suprasylvian cortex (Zumbroich & Blakemore, 1987) exhibit significantly broader spatial frequency tuning than that estimated from the masking experiments and measured in Area 17.

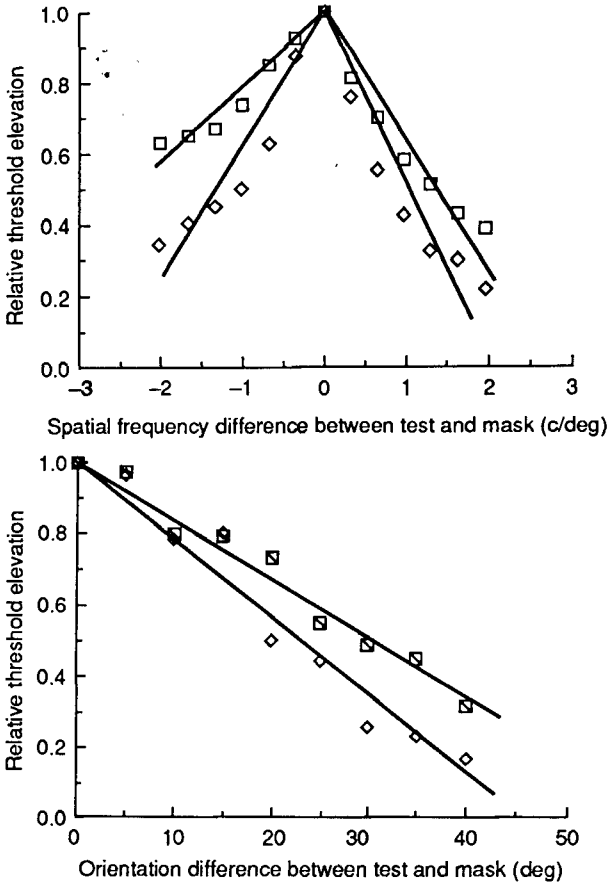

Fig. 4 (Top) □, 0.35 c/deg; ◆, 1.45 c/deg. Elevation in contrast threshold for detection of a grating pattern that appeared within a band of one-dimensional noise whose spatial frequency content was varied relative to the spatial frequency of the test grating. The units along the abscissa are octaves, where an octave is a factor of two difference in spatial frequency. (Bottom) ⍁, 0.35 c/deg; ◇, 1.0 c/deg. Elevation in contrast threshold for detection of a vertical grating appearing within a 1-octave band of noise whose orientation was varied relative to vertical. The values along the abscissa are angular degrees (e.g., a value of 45° corresponds to noise whose contours are oriented diagonally).

Turning next to orientation selectivity, the pair of curves in the bottom panel shows that noise impaired detection of the test grating only when the orientations of the test and noise were within 25–30° of one another. Furthermore, orientation selectivity was consistently narrower at higher spatial frequencies. These values, too, correspond quite well with estimates of orientation tuning for cortical cells (e.g., Rose & Blakemore, 1974). Because there is overlap in the degree of orientation tuning of cells in Areas 17 and 18, however, we cannot draw conclusions about the population of cortical cells (e.g., Area 17 versus Area 18) responsible for the orientation selectivity revealed by masking.

Comparable masking experiments have been performed on humans, and resulting estimates of spatial frequency tuning (Stromeyer & Julesz, 1972) and orientation selectivity (Campbell & Kulikowski, 1966; Phillips & Wilson, 1984; Black & Holopigian, 1985) very closely match the estimates derived for the cat. Some of those results from humans are discussed in Chapter 10. Suffice it to say, this equivalence between human and cat spatial vision point to the involvement of comparable neural mechanisms in grating resolution by humans and by cats.

E. Spatial Discrimination

The two previous subsections focused on tasks involving the *detection* of spatial patterns by the cat. Now let's consider how well the cat can *discriminate between* clearly visible, high-contrast patterns on the basis of orientation or spatial frequency. More to the point, can we predict the cat's discrimination from the spatial selectivity of single cortical neurons?

1. Orientation

Starting first with discrimination between targets which differ only in orientation, the smallest published behavioral threshold for the cat is 2° (Vandenbussche & Orban, 1983). Moreover, the cat (like man) shows an oblique effect for this discrimination, in that differences in grating orientations centered around vertical and horizontal are more finely discriminated than those centered around diagonal (Vandenbussche & Orban, 1983). In absolute terms, however, humans outperform cats: under optimum

conditions, humans can discriminate orientation differences as small as a fraction of a degree.

This species difference in orientation discrimination could be explained in several ways. First, cortical neurons in human visual cortex could be more narrowly tuned for orientation than neurons in cat cortex. Recall, however, that masking data (Blake & Holopigian, 1985) point to equivalent tuning in cat and human. Second, cat cortical neurons could be inherently more variable in their responsiveness, thereby requiring a larger change in orientation to yield a reliable response change. At present there is no way to evaluate this possibility. Finally, it could be that the cat's visual cortex, because it contains fewer neurons than the human visual cortex, samples the orientation domain more coarsely (Sakitt & Barlow, 1982). Because the standard error of the sum of N independent measures of a noisy process decreases as the square root of N, a visual cortex with more cells should resolve smaller angular differences. To make quantitative predictions about the expected size of this difference in discrimination thresholds between human and cat requires information (e.g., the dimensions of a hypercolumn in human vision) not currently available.

It is informative to compare the cat's behaviorally measured discrimination threshold with estimates of orientation tuning of cat cortical neurons. Estimates of orientation tuning vary, but even the most narrowly tuned neurons respond over a 40° range of orientations. Clearly, then, discrimination is not limited by the breadth of tuning. Bradley et al. (1987) have shown, though, that a reliable difference in the firing level of narrowly tuned cortical cells can be produced by an orientation difference as small as 1.84°, a value remarkably close to the best behavioral threshold. Bradley et al. point out that the ability of a single cell to signal these kinds of small orientation differences depends on the steepness of the cell's orientation tuning curve and the response variability of the cell.

2. Spatial Frequency Discrimination

To complete this survey of cat spatial vision, let us consider the animal's ability to discriminate patterns on the basis of differences in spatial frequency. For spatial frequencies near the peak of their contrast sensitivity function, cats can discriminate frequencies differing by as little as 20% (Blake, Holopigian & Wilson, 1986). Performance is worse at lower spatial frequencies, but this may have to do with the limited number of cycles actually contained in the test display. Once again, human performance on a comparable task is considerably better: at their best, humans can discriminate frequency differences of the order of 5% (e.g., Campbell, Nachmias & Jukes, 1970).

How well does the cat's behaviorally determined threshold compare to difference thresholds measured physiologically? Within their sample of 18 cat cortical cells, Bradley et al. (1987) found that the average spatial frequency difference reliably signaled was 21%, a value that matches the best performance observed behaviorally. It is noteworthy, though, that their sample of cells included a few that were sensitive to frequency differences as small as 5%, a value surpassing the cat's best performance but equaling the best performance exhibited by human observers. Again, the difference between cat and human discrimination performance may be related to the difference in the number of cells in their visual cortex, that is, the size of the basis set, to use a term borrowed from sampling theory (Sakitt & Barlow, 1982).

F. Conclusion

Cat and human spatial vision are comparable in several important ways. Both species can resolve spatial frequencies spanning about a 5-octave range, with the visible range for the cat situated at a point lower along the spatial frequency axis. When detecting grating patterns, both cats and humans appear to utilize neural channels narrowly tuned for spatial frequency and orientation. Where cat and human spatial vision are dissimilar (e.g., visual acuity), we can point to neuroanatomical differences between the two species (e.g., ganglion cell density) that may account for these dissimilarities in performance.

III. INSIGHTS INTO HUMAN COLOR VISION FROM STUDIES OF OTHER MAMMALS

Color vision is a much studied characteristic of our species. The keenness of the human color capacity and its role in visual perception have been documented in countless psychophysical experiments, and the literature burgeons with details as to how stimulus variation relates to perceived color. Yet, despite all of this effort, there is still only a very limited understanding of the biological mechanisms underlying human color vision. To achieve this understanding one must rely on examination of nonhuman visual systems. This section examines the advantages of studying other mammals as an aid to understanding human color vision and provides one example of how such an approach has proven fruitful. (See Chapter 8, this volume.)

A. General Comments on Color Vision in Mammals

Color vision has been demonstrated in most mammalian species for which compelling investigations have been carried out (for a review see Jacobs, 1981), and there is only a single mammalian species, the rat, for which the evidence indicates a complete lack of color vision capacity (Neitz & Jacobs, 1986b). However, color vision among mammals also varies considerably from humans both in acuteness (i.e., the fineness of color discrimination) and its dimensionality. With respect to the latter, only the primates have shown trichromatic color vision (i.e., color vision based on three cone receptor photopigments in the retina) like that of humans. Rather, most mammals have dichromatic vision (i.e., color vision based on two cone receptor pigments in the retina). This variation from the human color capacity can be turned to a research advantage in comparative color vision studies. Consider the following question: What implications for color vision arise from the spectral positioning and spectral separation of various cone types? An answer to this question would be of interest, both as an aid to understanding the details of chromatic opponent organizations and perhaps for giving insight into why particular cone types and combinations have evolved.

Dichromacy appears to be the normal color vision for many mammals. Among dichromatic mammals, however, the actual cone pigment complement varies considerably. For instance, although ground squirrels, tree squirrels, and tree shrews all have short wavelength cones with roughly the same spectral peaks (435–445 nm), these three species show great variation in the spectral location of their second longer wavelength cone—from 518 to 556 nm (Jacobs, Neitz & Crognale, 1985; Jacobs & Neitz, 1986; Blakeslee, Jacobs & Neitz, 1988). A comparison of the response properties of the spectrally opponent units in the visual systems of these three species could be used to illuminate the advantages and disadvantages for color vision associated with variation in the pairings of different cone pigment sets.

Mechanisms of color vision vary considerably among species, and some nonmammalian vertebrates are known to have good color vision. One might suppose that these species would provide better models for understanding human color vision than the mammals who, as we have noted, mostly do not have very keen color vision. However, problems arise from some very obvious differences in mechanisms used to produce color vision in mammals and nonmammals. Three such differences may be noted: (a) A large number of nonmammalian species, for instance many birds and reptiles, employ an elaborate system of color oil droplets which, in conjunction with multiple classes of cone pigments, provide an initial filtering of spectral input quite unlike that found in humans or any other mammals. (b) The great expansion of the neocortex of mammals means that the central visual projections differ fundamentally between mammals and nonmammals, and, thus, the central nervous system mechanisms for elaborating color information are also quite different. (c) It appears that the means for organizing spectrally opponent pathways may be fundamentally different in mammalian and nonmammal-

ian visual systems. In the latter, at least in certain fishes, birds, and reptiles, the connections between specific cone types and horizontal cells appear rigidly deterministic, whereas in mammalian retinas no evidence for such a specificity of connection is apparent (Boycott, Hopkins & Sperling, 1987). The opponent separation required to produce color vision must, thus, arise quite differently in mammalian and nonmammalian visual systems. All of these features suggest that although many species have color vision capacity, the machinery for its accomplishment varies considerably. That variation appears smaller within mammals than between mammals and other vertebrates.

B. Polymorphism of Color Vision in a Nonhuman Primate

We turn now to an example of the thesis proposed above; that is, a description of a case where the study of color vision in a nonhuman species has significant implications for understanding human color vision. It has long been recognized that color sensitivity varies considerably among humans, namely, there are different forms of color sensitivity, which are best known as the familiar color vision defects and anomalies. The study of atypical color vision cases has been central in many attempts to understand the mechanism for human color vision. Since the mid-1970s it has been discovered that other primate species also have color sensitivities which systematically differ from normal human color sensitivity. This is significant, because in these species the mechanism underlying the different forms of color vision can be directly examined. One such species is the squirrel monkey (*Saimiri sciureus*).

The polymorphism of squirrel monkey color vision was discovered with behavioral tests of the same sort used to reveal polymorphisms of human color vision (Jacobs, 1983a,b, 1984). Figure 5 summarizes results from several behavioral tests on individual squirrel monkeys and illustrates the magnitude of these differences. In formal classification, some monkeys would

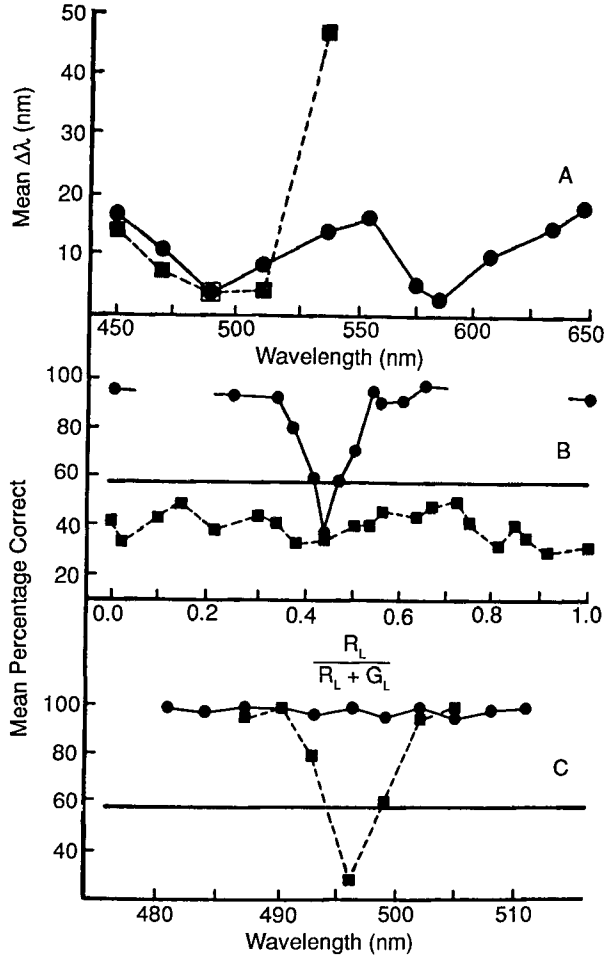

Fig. 5 Examples of results obtained from a dichromatic squirrel monkey (squares) and a trichromatic squirrel monkey (circles) on three tests of color vision. (A) Wavelength discrimination functions. (B) Rayleigh matches. In this test animals were required to discriminate various mixtures of red and green lights from a standard yellow light. The data points are the performance levels obtained from highly trained animals in a three-alternative discrimination task. The horizontal line indicates the 95% confidence level for successful discrimination. Note that the dichromatic animal is unable to make any of the color discriminations. (C) Tests for the presence of a neutral point. In this test animals were required to discriminate monochromatic lights from an equiluminant achromatic light. Other details are the same as for B. (From Jacobs & Neitz, 1985.)

be considered to have trichromatic color vision, and others have dichromatic color vision. Furthermore, just as in the case of the human color vision polymorphism, several subtypes can be discerned in each of these categories. The total range of color vision variation in a large sample of squirrel monkeys encompassed six types; three of these were trichromatic variants and three dichromatic (Jacobs, 1984). Not only does the squirrel monkey share the human characteristic of color vision polymorphism, but also some of the variants appear qualitatively similar. For instance, some squirrel monkeys behaved similarly to human protanopes in sensitivity to the long wavelengths, wavelength discrimination abilities, and color matching.

What accounts for the strikingly different forms of squirrel monkey color vision? To examine this question, measurements of cone photopigments were made in squirrel monkeys whose color vision had been established by behavioral tests (Mollon, Bowmaker & Jacobs, 1984; Bowmaker, Jacobs, Spiegelhalter & Mollon, 1985; Bowmaker, Jacobs & Mollon, 1987). Photopigments were measured with microspectrophotometry (MSP), a procedure that involved the passage of a narrow measuring beam through the outer segments of individual photoreceptors. MSP measurements were made on photoreceptors from a total of 16 squirrel monkeys. From this group of animals absorbance spectra were obtained for more than 600 individual cones.

Five different classes of photoreceptors were found in this sample of squirrel monkeys. One class, having an average peak sensitivity (λ_{max}) at about 498 nm, represents rods, while the other four classes represent cones. One sparsely represented type of cone in these retinas had an average λ_{max} of about 433 nm. The average λ_{max} values for the other three were 536, 549, and 564 nm. Unlike the rods and short wavelength cones, there were striking variations in the presence of these three cone types among the individual animals. That variation corresponded exactly with the measured variation in color vision.

Figure 6 shows spectral sensitivity functions based on the absorbance of the four cone pigments of squirrel monkeys. Animals with dichromatic color vision have either the 536, 549, or 564 nm cone pigments, each in conjunction with the 433 nm cone pigment. Those monkeys with trichromatic vision may have any pair of the three longer wavelength cone pigments in conjunction with the 433 nm cone pigment, that is, 536 and 549 nm, or 549 and 564 nm, or 536 and 564 nm cone pigments.

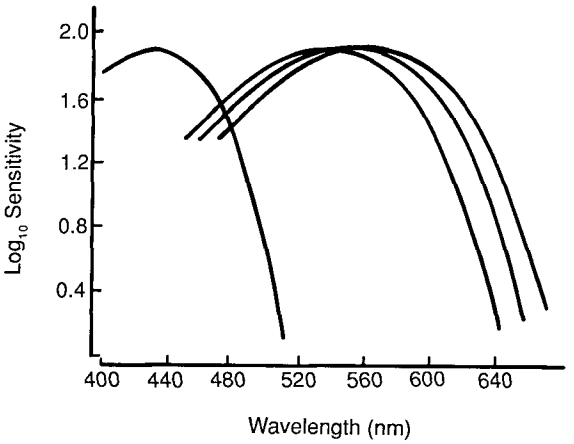

Fig. 6 Smoothed and normalized absorbance curves for the four classes of cone pigment found in the squirrel monkey. These pigments are present in various combinations in individual animals (see text).

The results illustrated in Figs. 5 and 6 indicate that the different forms of color vision in a nonhuman primate, the squirrel monkey, depend entirely on parallel differences in the complement of cone pigments. There are several implications of this discovery for understanding the mechanisms that underlie human color vision.

C. Squirrel Monkey Color Vision: Implications for Human Color Vision

For some issues, the study of squirrel monkey color vision and its mechanisms can make long-held ideas about the mechanisms for human color vision either more or less plausible, but in other cases, new explanations may be suggested. Examples of both follow.

1. Color Vision Variations Due to Photopigment Variations

It has long been believed that the major forms of congenital color vision defects in humans arise from variations in the cone pigments. For example, dichromacy reflects the absence of one of the three normal cone classes (e.g., Boynton, 1979; Pokorny, Smith, Verriest & Pinckers, 1979). That view has been supported by many indirect measurements which were strongly believed to reflect the function of the cone pigments, namely, color matching, measurements of visual sensitivity, reflection densitometry, etc. (Alpern & Pugh, 1977; Alpern & Wake, 1977). However, only in a few cases has it been possible to measure directly cone pigments in individuals whose color vision differed in known ways (Weale, 1959; Baker & Rushton, 1965). The discovery that the cone pigment complements of squirrel monkeys discretely differ, in parallel with their measured differences in color vision, shows clearly that the explanation for variations of human color vision accurately accounts for color vision variations in another primate. As such, that result supports the belief that the major forms of human color vision variation can be traced to individual differences in the cone pigment complement.

2. Explanations for Anomalous Trichromacy

The anomalous trichromacies represent both the most frequent of the congenital color vision variations in humans and the most difficult to explain. Over the years a considerable number of hypotheses have been advanced to account for these anomalies (Pokorny et al., 1979).

Psychophysically, there are three trichromatic phenotypes among squirrel monkeys (Jacobs, 1984). They have been defined in terms of the relative proportions of a red + green mixture required to "match" a standard yellow light. One of the three groups required roughly the same proportions of red and green as a normal human trichromat, but the other two groups behaved somewhat similarly to the two major forms of human anomalous trichromatism, that is, one required relatively more red light in the mixture while the other required relatively more green light. Although the correspondence is by no means perfect (see Bowmaker et al., 1985), a reasonable analogy can be drawn between these latter two squirrel monkey phenotypes and anomalous human color vision.

This analogy sheds light on some of the explanations advanced for human anomalous trichromacy. For instance, it has been suggested that human anomalous trichromacy might result from abnormal variations in optical density of the cone pigment (Ruddock & Naghshineh, 1974) or in the mixing together in a single receptor of two types of photopigment (Baker, 1966). To the contrary, the squirrel monkey trichromatic variations seem to result exclusively from discrete shifts in the spectra of the cone pigments (Fig. 6); there is no evidence either for variation in pigment density or for mixing of pigments within a single receptor. Therefore, these explanations for anomalous trichromacy are rendered much less plausible.

3. Photoreceptor Mosaics in Heterozygous Females

Human color vision defects and anomalies are unequally represented in the two sexes. A similiar distribution of the different forms of color vision can be found in the squirrel monkey. Whereas female squirrel monkeys have been found to have either trichromatic or dichromatic color vision, all male monkeys are dichromats (Jacobs, 1984). This finding has led to the hypothesis that the inheritance of middle to long wavelength cone pigments in squirrel monkeys is produced by the action of three alleles (form of a gene on a chromosome) at a single locus on the X chromosome (Mollon et al., 1984; Jacobs & Neitz, 1985). Each allele accounts for one of the three middle to long wavelength cone pigments. Such an arrangement would account for the universality of dichromacy among males. The hypothesis further supposes that random X-chromosome inactivation occurs in female monkeys, thus allowing the heterozygous animal to have two populations of middle to long wavelength cones. This provides the basis for trichromatic color vision. There is now substantial evidence indicating

that this mechanism correctly accounts for the different forms of color vision in the squirrel monkey (Jacobs & Neitz, 1987).

It has long been supposed that in the human, unlike the squirrel monkey, there are two (or more) cone pigment genes on the X chromosome with the middle to long wavelength cone pigments specified at these loci (see Nathans, 1987). Classical theory further suggests that low frequency alleles at these loci specify aberrant photopigments; these will be directly expressed in males, leading to the common forms of color anomaly and color defect. The mother or female child of such a male defective will be heterozygous at a pigment locus, and such individuals will presumably produce an aberrant photopigment in addition to two normal photopigments. In heterozygous females, random X–chromosome inactivation would be expected to lead to a retinal cone mosaic in which some cones express maternally derived chromosomes while others express paternally derived chromosomes. There have been a number of attempts to demonstrate cone mosaicism in heterozygous females (Pokorny et al., 1979), but consistent evidence for the presence of such is lacking.

The results from the squirrel monkey suggest that it may be difficult to demonstrate photoreceptor mosaicism in heterozygous females because the mosaics formed by paternally and maternally derived photoreceptors have a relatively fine grain. There are two arguments in support of this possibility. First, simply to produce trichromacy in the female squirrel monkey, the two middle-to-long-wavelength pigments would each have to be present in regions no larger than the dimensions of individual retinal receptive fields. Second, and perhaps more directly, MSP examination of arrays of 1–2 dozen neighboring photoreceptors from the foveal tissue of a trichromatic squirrel monkey revealed no evidence that the two cone types were systematically arranged into a mosaic pattern (Mollon et al., 1984). Rather, the two cone types seemed to be randomly intermixed. In sum, work with the squirrel monkey suggests that photoreceptor arrays formed by random X-chromosome inactivation are fairly fine grained. This may well be why the presence of such mosaics has been hard to demonstrate in the human heterozygous female.

IV. COLOR VISION IN GOLDFISH: A MODEL FOR HUMAN COLOR VISION?

Color vision is assumed to be adapted to the specific environmental conditions under which an animal lives. The number and spectral sensitivities of the receptor types and the neural organization of the visual system can differ widely across species. Therefore, it seems rather unlikely to find close similarities between color vision systems in humans and animals from different habitats. However, if two color vision systems that have evolved independently reveal similar properties, then general functional principles for the design of any highly effective color vision system may be invoked. For example, color vision in the honeybee is trichromatic, and it resembles human color vision in wavelength discrimination as well as in color contrast and color constancy (von Helversen, 1972; Neumeyer, 1980, 1981). It has a spectral sensitivity function, however, that is different from humans, with a shift into the ultraviolet (UV), and is located between 300 and 650 nm. Whether color vision of the honeybee has the properties of an opponent color vision system, as found in humans (see Chapter 8, this volume), or whether it is more simply organized is still an open question. In vertebrates, highly effective color vision systems based on more than two cone types, and possibly as many as four, are found in fishes, reptiles, and birds (Jacobs, 1981).

A. Why the Goldfish as an Experimental Animal?

Goldfish, carp, and other cyprinid fishes have long been important subjects in studies of photoreceptor cells, retinal physiology, and structure. Early microspectrophotometric measurements of single cone outer segments in the goldfish revealed absorption spectra

of three types of photopigments (Marks, 1965), and the first intracellular recordings of vertebrate photoreceptors showed three spectral types of cones in the carp (Tomita, 1965). The results of neurophysiological and neuroanatomical investigations indicated that the cyprinid retina is a highly complicated structure in which important steps of color specific information processing take place (Wheeler, 1982). Investigations of single cones in the goldfish have shown three spectral types with maximal sensitivities at 450, 535, and 620 nm. This, together with the fact that retinal neurons have response properties of "color opponency" as in the primate visual system, suggested that goldfish might have a trichromatic color vision system similar to that of humans.

The perceptual properties of color vision can only be investigated in behavioral experiments. The behavioral testing technique, in which a presentation of color is rewarded with food, was introduced by Karl von Frisch (1913, 1914) to study color vision in the minnow, a cyprinid fish, and in the honeybee. In lower vertebrates, however, this method has been only rarely applied and investigations of color vision in these species have been largely neglected.

B. The Measurement of Wavelength Discrimination

To characterize a color vision system, an understanding of differential wavelength discrimination ($\Delta\lambda$) is of central importance. The $\Delta\lambda$ function can provide insight into the number of photoreceptor types involved and the peripheral steps of information processing. Early measurements of wavelength discrimination were obtained by Wolff (1925) in the minnow (*Phoxinus laevis*) and later in the goldfish by Yarczower and Bitterman (1965). Both experiments failed to equate the color stimuli in brightness for the fish, so discriminations may have been based on either brightness *or* hue. Therefore, wavelength discrimination in the goldfish was reexamined using the following method (Neumeyer, 1986). Freely swimming goldfish could choose between two test fields illuminated by monochromatic light. Choice of the correct color was rewarded with a small amount of a food paste delivered through thin plastic tubes at the test field (see Fig. 7). Test fields were illuminated using slide projectors and fiber optics. The intensity of the monochromatic light was adjusted to equal stimu-

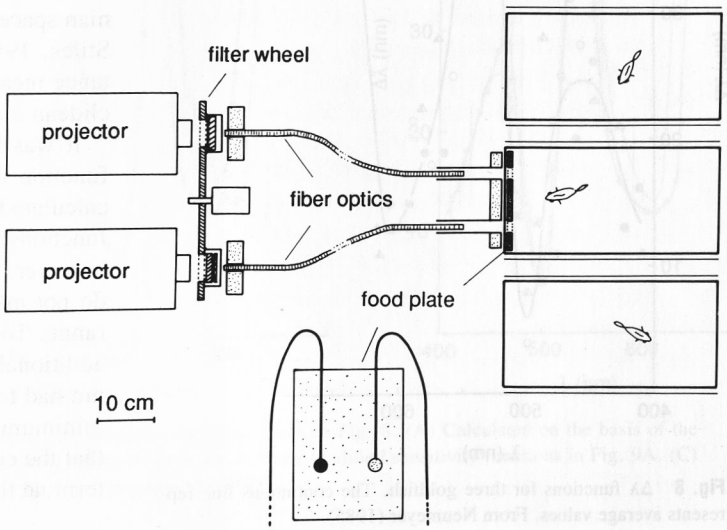

Fig. 7 Experimental setup for wavelength discrimination experiments. The three identical tanks with single goldfish are seen from the top. The optical apparatus could be moved from one tank to the other. The filter wheel contained interference and neutral density filters. The food plate was inserted into the water and contained the two test fields which were illuminated from the outside of the tank. A food paste was given for reward through thin tubes which ended at the test field openings. When measuring spectral sensitivity, the fish was trained to swim to the nonilluminated (dark) test field while the comparison test field was illuminated with monochromatic light of different wavelengths and intensity. In the measurement of wavelength discrimination, the two test fields were illuminated with monochromatic light of different wavelengths, with intensities adjusted to equal "fish-subjective" brightness according to their spectral sensitivity function.

lus efficiency, according to the spectral sensitivity function measured previously under the same experimental conditions (Neumeyer, 1984). The fish were trained using 20 wavelength pairs between 404 and 719 nm. The frequency with which the training wavelength was approached relative to the comparison wavelength was determined. The difference threshold for the two wavelengths ($\Delta\lambda$) was defined as a choice frequency of 70%.

Figure 8 shows the $\Delta\lambda$ function of the goldfish. Small values of $\Delta\lambda$, indicating a keen wavelength discrimination, were found at 400, 500, and 610 nm. This result is surprising, as in other trichromatic color vision systems there are only two ranges of best wavelength discrimination.

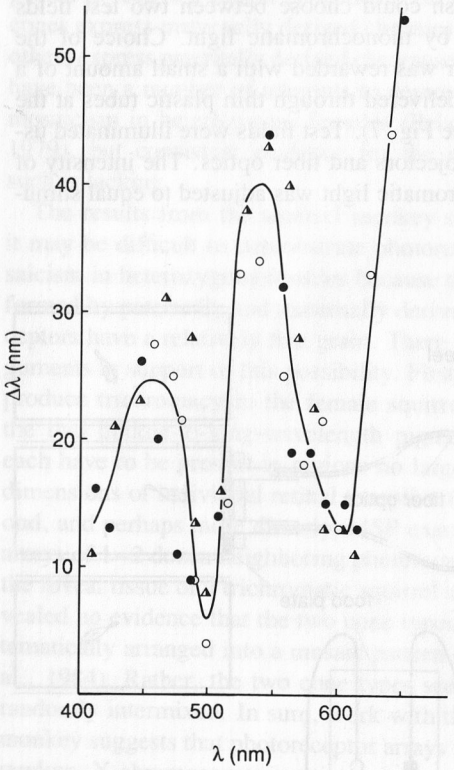

Fig. 8 $\Delta\lambda$ functions for three goldfish. The continuous line represents average values. From Neumeyer (1985).

To understand the processes underlying wavelength discrimination, model computations of the $\Delta\lambda$ function were performed based on the following considerations (for details see Neumeyer, 1986). In the response of a single cone, information about wavelength is lost (i.e., excitation is proportional only to the number of quanta absorbed). To obtain information about "color," the central nervous system has to compare the excitation values of at least two classes of cones having different spectral sensitivities. The effect of each wavelength on the different cone types represents the "input side" of the color vision system, and this effect can be described by a point in color space. The coordinates of this point (color locus) stand for the relative excitation values of the three cone types. The color loci of two wavelengths which can "just be discriminated" by the animal have a distance **R** in color space. According to Helmholtz (1892), this distance is equal for each just discriminable wavelength pair. When **R** is calculated for one such experimentally determined pair, it is possible to ask for each other wavelength, which adjacent wavelength has the same distance **R**. The difference between these two wavelengths is $\Delta\lambda$. To calculate **R**, the metrics of the color space must be defined. In human color vision, Helmholtz (1892) proposed that **R** can be calculated as the line element in the Riemannian space, as the most general case (see Wyszecki & Stiles, 1982). In the goldfish, a special case of distance measure was used; **R** was calculated as the euclidean distance.

It was first determined whether the measured $\Delta\lambda$ function of the goldfish is similar to a $\Delta\lambda$ function calculated on the basis of the animal's cone sensitivity functions, as shown in Fig. 9. Figure 10A shows, however, that the measured and theoretical functions do not match, especially not in the short wavelength range. To obtain small values of $\Delta\lambda$ in this range, an additional sensitivity increase between 400 and 450 nm had to be assumed. Several attempts to model the minimum at 610 nm failed and led to the hypothesis that the cone sensitivity functions do not uniquely determine the $\Delta\lambda$ function (see below).

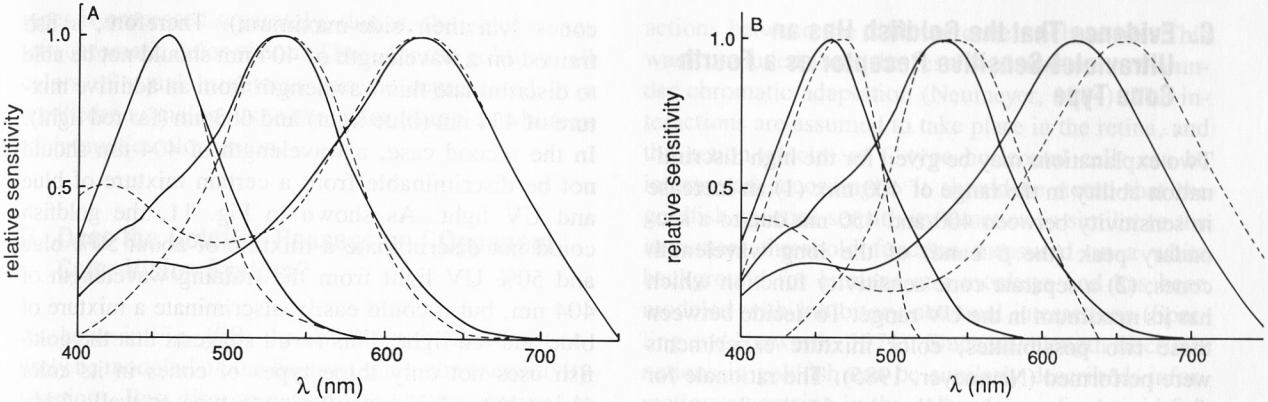

Fig. 9 Spectral sensitivity functions that were used in the model computations of the Δλ function. Continuous lines: Cone spectral sensitivity functions as obtained in direct measurements of photopigment absorption spectra. (The calculated Δλ function based on these functions is shown in Fig. 10A.) Dashed lines: Modified sensitivity functions. (A) Functions which approximated the measured Δλ function in the short and the mid-wavelength spectral range (Fig. 10B). (B) Functions which gave the best approximation in the entire spectral range (Fig. 10C). From Neumeyer (1986).

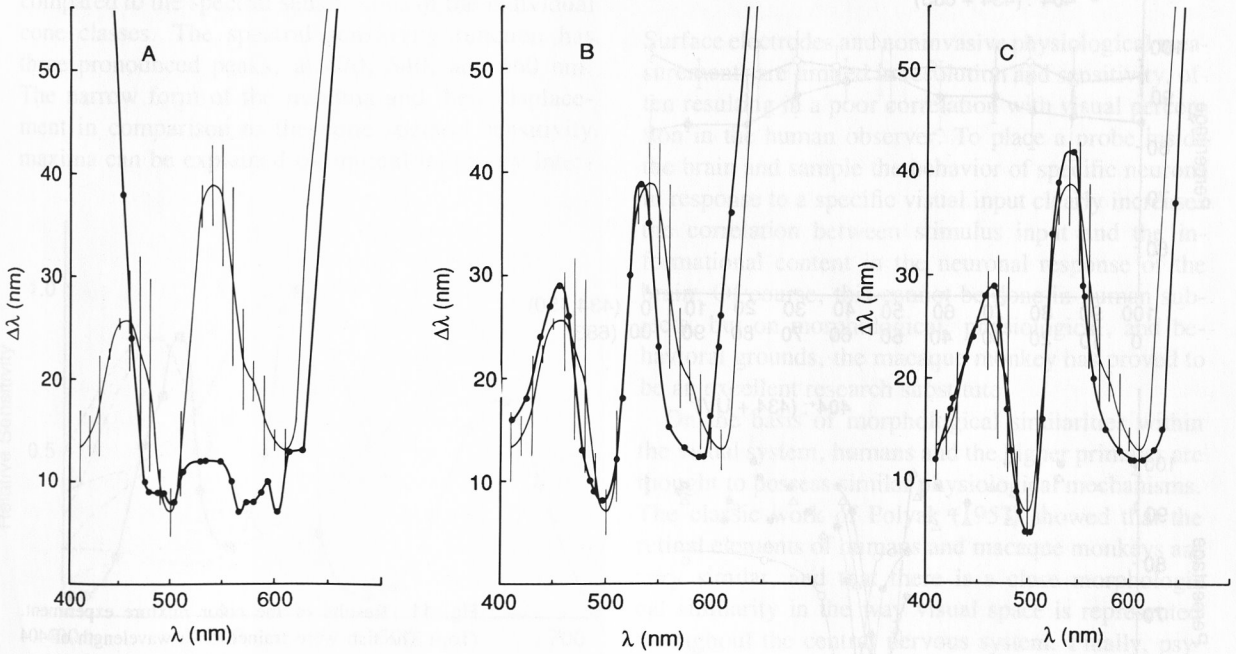

Fig. 10 Calculated Δλ functions (dots) in comparison to the measured Δλ function from Fig. 8. (A) Calculated on the basis of the cone sensitivity functions (continuous lines in Fig. 9). (B) Calculated on the basis of the modified sensitivity functions in Fig. 9A. (C) Calculated on the basis of the modified functions in Fig. 9B. From Neumeyer (1986).

C. Evidence That the Goldfish Has an Ultraviolet-Sensitive Receptor as a Fourth Cone Type

Two explanations may be given for the high discrimination ability in the range of 400 nm: (1) an increase in sensitivity between 400 and 450 nm due to a secondary peak (the β band) of the long wavelength cones; (2) a separate cone sensitivity function which has its maximum in the UV range. To decide between these two possibilities, color mixture experiments were performed (Neumeyer, 1985). The rationale for the procedure was the following: In the first case, short wavelength light of 404 nm should excite the short wavelength cones as well as the long wavelength cones (via their side-maximum). Therefore, a fish trained on a wavelength of 404 nm should not be able to discriminate this wavelength from an additive mixture of 434 nm (blue light) and 683 nm (far red light). In the second case, a wavelength of 404 nm should not be discriminable from a certain mixture of blue and UV light. As shown in Fig. 11, the goldfish could not discriminate a mixture of about 50% blue and 50% UV light from the training wavelength of 404 nm, but it could easily discriminate a mixture of blue and red light. This result suggests that the goldfish uses not only three types of cones in its color vision but a UV-sensitive cone type as well. Additional color mixture experiments have shown (Neumeyer, 1988) that the information from the four cone

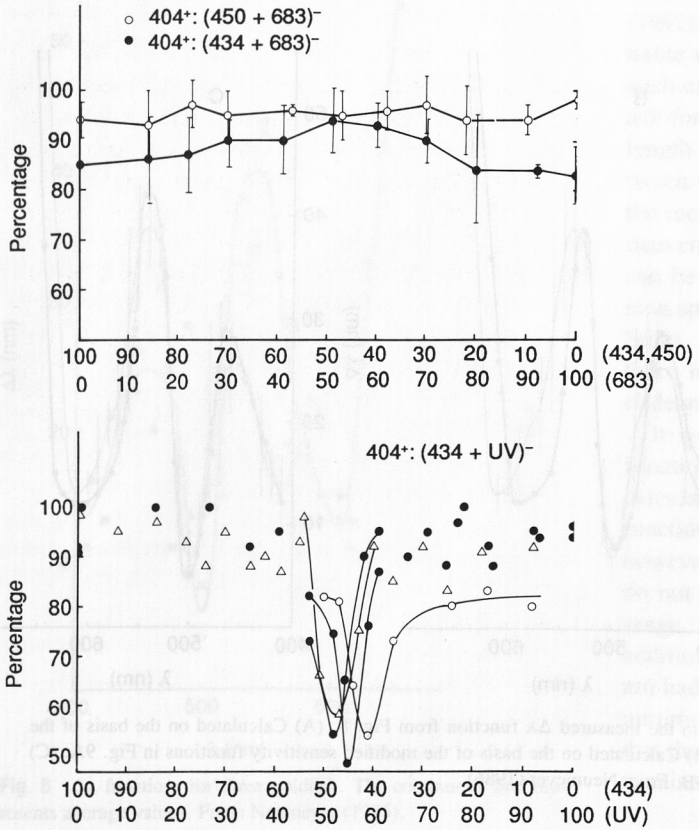

Fig. 11 Results of the color mixture experiment. (Top) The fish were trained on a wavelength of 404 nm and tested against an additive mixture of blue light (450 nm) and far red light (683 nm). (Bottom) Trained as above, but tested against a mixture of blue light (434 nm) and ultraviolet (367 nm) light. Different symbols denote results from different animals.

types is processed separately, that is, the goldfish has tetrachromatic color vision. Thus, for the goldfish, all colors of equal brightness can be represented in a tetrahedron, analogous to the color triangle of human trichromatic color vision.

D. Does the Goldfish Possess an "Opponent" Color Vision System?

As shown in Fig. 10B, the $\Delta\lambda$ function could not entirely be modeled on the basis of three cone sensitivity functions. Best discrimination was always obtained at shorter wavelengths (590 instead of 610 nm). Only when the maximum of long wavelength cone sensitivity was shifted to 660 nm could a good approximation be obtained (Fig. 10C).

Figure 12 shows behavioral measures of goldfish spectral sensitivity measured from 400 to 719 nm compared to the spectral sensitivities of the individual cone classes. The spectral sensitivity function has three pronounced peaks, at 470, 540, and 660 nm. The narrow form of the maxima and their displacement in comparison to the cone spectral sensitivity maxima can be explained by mutual inhibitory interactions between the different cone mechanisms. This was concluded from the results of measurements under chromatic adaptation (Neumeyer, 1984). The interactions are assumed to take place in the retina, and the action spectra of C-type horizontal cells can be interpreted accordingly. It should be noted that the goldfish spectral sensitivity function is similar to the increment threshold function measured on a white background for humans and monkeys and has been modeled with inhibitory neuronal interactions (Sperling and Harwerth, 1971). Since wavelength discriminations in goldfish can be similarly described, information processing in the color vision of cyprinid fish might be similar to that in primate visual systems.

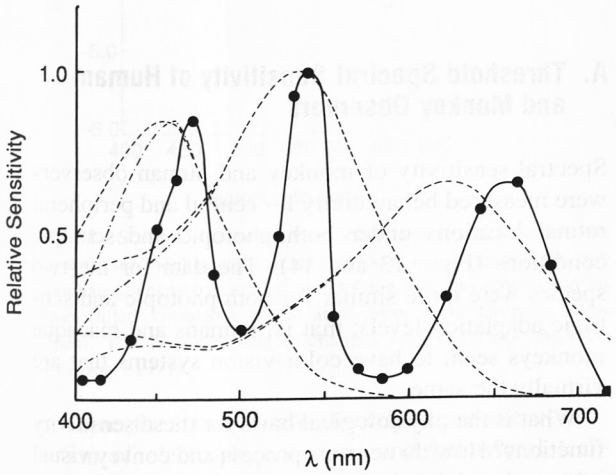

Fig. 12 Relative spectral sensitivity function of the goldfish (dots) in comparison with the sensitivity functions of cones (dashed lines, after Harosi, 1976). From Neumeyer (1984).

V. SPECTRAL SENSITIVITY OF HUMANS, RHESUS MONKEYS, AND NEURONS

Surface electrodes and noninvasive physiological measurements are limited in resolution and sensitivity, often resulting in a poor correlation with visual perception in the human observer. To place a probe inside the brain and sample the behavior of specific neurons in response to a specific visual input clearly increases the correlation between stimulus input and the informational content in the neuronal response of the brain. Of course, this cannot be done in human subjects, but on morphological, physiological, and behavioral grounds, the macaque monkey has proved to be an excellent research substitute.

On the basis of morphological similarities within the visual system, humans and the higher primates are thought to possess similar physiological mechanisms. The classic work of Polyak (1957) showed that the retinal elements of humans and macaque monkeys are very similar, and that there is a close morphological similarity in the way visual space is represented throughout the central nervous system. Finally, psychophysical comparisons between macaque monkeys and human observers have shown striking similarities in the vision of the two species (Blough & Schrier, 1963; Sidley & Sperling, 1967; DeValois & Jacobs,

1968; DeValois, Morgan, Polson, Mead & Hull, 1974; Crawford, 1976, 1977; Harwerth & Smith, 1985; Oehler, 1985; Spillmann, Ransom-Hogg & Oehler, 1987). In short, the macaque monkey (in particular, the rhesus monkey, *Macaca mulatta*) appears to meet all criteria as a psychophysical, anatomical, and physiological research surrogate for the human visual system.

Even though the psychophysical evidence on the comparability between the visual capacities of the macaque and human has been compelling, data have been presented for only a small number of experimental conditions. Color or spectral sensitivity data for the macaque monkey has been shown to be similar to that of humans under photopic levels of light adaptation (Grether, 1939; Sidley & Sperling, 1967; DeValois & Jacobs, 1968; Sperling, Sidley, Dockens & Jolliffe, 1968; DeValois et al., 1974; Harwerth & Smith, 1985), while Blough and Schrier (1963) demonstrated similar scotopic sensitivities in the two species. However, these data were obtained without control over where the test flash fell upon the retina. Moreover, with the exception of the work by Sperling, the test stimuli have been projected on reflective or rear-projection surfaces, thus making it difficult to compare monkey sensitivity with that of man on an absolute quantum scale. The use of a Maxwellian-view optical system (Sidley, Sperling, Bedarf & Hiss, 1965) obviates this problem. Finally, with development of additional behavioral procedures to control fixation (Crawford, 1976, 1977) spectral sensitivities can be obtained for a variety of retinal loci and under a variety of luminance and chromatic adaptation conditions.

Fixation control, increment-threshold measurement, and microelectrode recording from single neurons have been combined to study the visual signals from the lateral geniculate nucleus (LGN) to the cortex when the monkey is responding to the visual stimulus. These combined techniques have permitted the *perceptive field* (Jung & Spillmann, 1970) of the alert behaving monkey to be brought into spatial registry with the *receptive field* of the LGN neuron. The neuronal receptive field was conventionally defined as the area of the retina (and visual space) that, when stimulated, produced a change in the response rate of the neuron. The perceptive field, on the other hand, referred to the area of the retina (and visual space) that, when stimulated by a visual stimulus, produced a change in the behavioral response of the monkey. Therefore, both the monkey and the neuron alike could be instructed: "Tell us if you can see the test flash." By systematically reducing (in 0.2 log-unit steps) the number of quanta contained in the test flash, the threshold sensitivities of the monkey and the neuron were determined for 22 wavelengths across the visible spectrum, each at the same retinal locus and under the same viewing conditions, and in the absence of any confounding effects of anesthesia.

Threshold for the monkey was operationally defined as the log of the reciprocal of the number of quanta contained in a test flash detected half the time. Similarly, threshold for the neuron was defined as the number of quanta in the test flash that evoked a "just observable change" in response rate of the neuron compared to the ongoing spontaneous discharge rate. This could be either an increase or decrease in response rate, as color-opponent neurons were often encountered, responding with excitation to stimulation with one wavelength of the test flash and with response inhibition to a different wavelength.

A. Threshold Spectral Sensitivity of Human and Monkey Observers

Spectral sensitivity of monkey and human observers were measured behaviorally for central and peripheral retinal locations under both photopic and scotopic conditions (Figs. 13 and 14). The data for the two species were quite similar for both photopic and scotopic adaptation levels; that is, humans and macaque monkeys seem to have color vision systems that are virtually the same.

What is the physiological basis for these sensitivity functions? How do neurons process and convey visual information throughout the visual system? And, what information does a single neuron convey about the colors of objects of the visual world? It is possible to

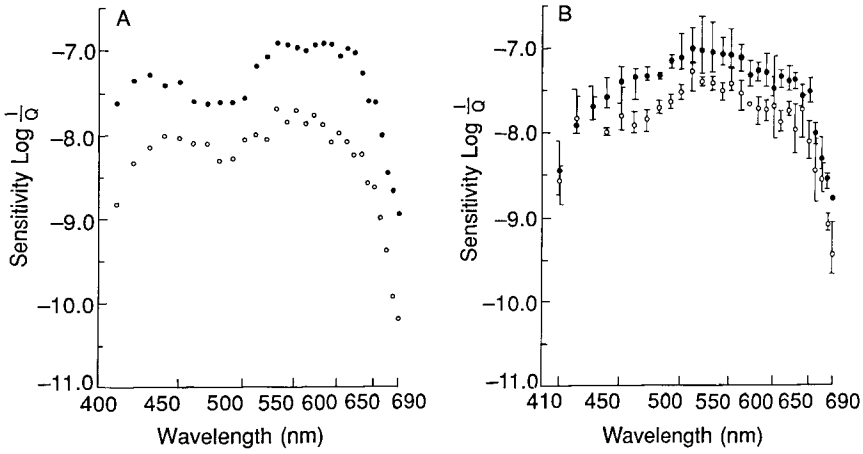

Fig. 13 (A) Photopic increment-threshold spectral sensitivity curves for a human observer taken at center fovea (filled) and at 14° away in the temporal retina (open). Note that there is a drop of about 1.0 log unit in sensitivity, with only minor differences in the shapes of the curves. (B) Photopic increment-threshold spectral sensitivity curves for a rhesus monkey taken under identical conditions as for (A). Note that the peak threshold sensitivity of the monkey is virtually identical to that of the human observer, and that the shape and drop in sensitivity with peripheral viewing are quite comparable to the human.

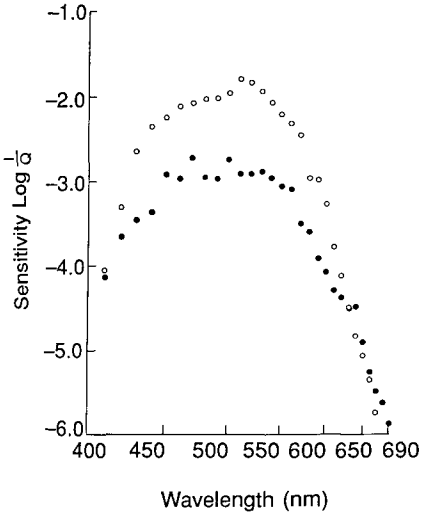

Fig. 14 Scotopic increment-threshold spectral sensitivity curves for a rhesus monkey for two retinal locations. Note that the rod-dominated sensitivity curve is about 1 log unit less sensitive in the fovea (filled) compared to that at 6° away in the temporal retina (open). This is comparable to changes seen in human observers (Crawford, 1977).

examine the visual brain directly using the combination of electrophysiological and behavioral techniques for insight as to how these mechanisms operate at the single-cell level to generate these behavioral functions.

B. Threshold Spectral Sensitivity of Monkey and Neurons

Rhesus monkeys were implanted with a stainless steel cylinder which accepted a head-mounted stereotaxic holder (Evarts, 1966). Varnished tungsten microelectrodes were then driven to the LGN of the alert behaving monkey by a micrometer-activated hydraulic system. Single neurons were isolated, and thresholds for monochromatic test flashes were measured for 22 wavelengths over the visible spectrum. Neurons were occasionally held for several hours, though responses (and thresholds) for single neurons were usually recorded for only a few minutes each. The tactic was to locate the receptive field for an LGN neuron and then, by shifting the fixation point, bring the perceptive field of the monkey into spatial registry so that both monkey and LGN neuron were "attending" to the same stimulus. The test stimulus was then reduced in intensity until the threshold was reached for the neuron and for the monkey (see Sperling et al., 1978).

The center of the receptive field of the LGN neuron was located by moving the fixation target in small steps and using a large 6° diameter test light, usually of 620 nm and high intensity. The experimenter rapidly covered the 18° field for a number of positions of the fixation target. The test light was then reduced to

1968; DeValois, Morgan, Polson, Mead & Hull, 1974; Crawford, 1976, 1977; Harwerth & Smith, 1985; Oehler, 1985; Spillmann, Ransom-Hogg & Oehler, 1987). In short, the macaque monkey (in particular, the rhesus monkey, *Macaca mulatta*) appears to meet all criteria as a psychophysical, anatomical, and physiological research surrogate for the human visual system.

Even though the psychophysical evidence on the comparability between the visual capacities of the macaque and human has been compelling, data have been presented for only a small number of experimental conditions. Color or spectral sensitivity data for the macaque monkey has been shown to be similar to that of humans under photopic levels of light adaptation (Grether, 1939; Sidley & Sperling, 1967; DeValois & Jacobs, 1968; Sperling, Sidley, Dockens & Jolliffe, 1968; DeValois et al., 1974; Harwerth & Smith, 1985), while Blough and Schrier (1963) demonstrated similar scotopic sensitivities in the two species. However, these data were obtained without control over where the test flash fell upon the retina. Moreover, with the exception of the work by Sperling, the test stimuli have been projected on reflective or rear-projection surfaces, thus making it difficult to compare monkey sensitivity with that of man on an absolute quantum scale. The use of a Maxwellian-view optical system (Sidley, Sperling, Bedarf & Hiss, 1965) obviates this problem. Finally, with development of additional behavioral procedures to control fixation (Crawford, 1976, 1977) spectral sensitivities can be obtained for a variety of retinal loci and under a variety of luminance and chromatic adaptation conditions.

Fixation control, increment-threshold measurement, and microelectrode recording from single neurons have been combined to study the visual signals from the lateral geniculate nucleus (LGN) to the cortex when the monkey is responding to the visual stimulus. These combined techniques have permitted the *perceptive field* (Jung & Spillmann, 1970) of the alert behaving monkey to be brought into spatial registry with the *receptive field* of the LGN neuron. The neuronal receptive field was conventionally defined as the area of the retina (and visual space) that, when stimulated, produced a change in the response rate of the neuron. The perceptive field, on the other hand, referred to the area of the retina (and visual space) that, when stimulated by a visual stimulus, produced a change in the behavioral response of the monkey. Therefore, both the monkey and the neuron alike could be instructed: "Tell us if you can see the test flash." By systematically reducing (in 0.2 log-unit steps) the number of quanta contained in the test flash, the threshold sensitivities of the monkey and the neuron were determined for 22 wavelengths across the visible spectrum, each at the same retinal locus and under the same viewing conditions, and in the absence of any confounding effects of anesthesia.

Threshold for the monkey was operationally defined as the log of the reciprocal of the number of quanta contained in a test flash detected half the time. Similarly, threshold for the neuron was defined as the number of quanta in the test flash that evoked a "just observable change" in response rate of the neuron compared to the ongoing spontaneous discharge rate. This could be either an increase or decrease in response rate, as color-opponent neurons were often encountered, responding with excitation to stimulation with one wavelength of the test flash and with response inhibition to a different wavelength.

A. Threshold Spectral Sensitivity of Human and Monkey Observers

Spectral sensitivity of monkey and human observers were measured behaviorally for central and peripheral retinal locations under both photopic and scotopic conditions (Figs. 13 and 14). The data for the two species were quite similar for both photopic and scotopic adaptation levels; that is, humans and macaque monkeys seem to have color vision systems that are virtually the same.

What is the physiological basis for these sensitivity functions? How do neurons process and convey visual information throughout the visual system? And, what information does a single neuron convey about the colors of objects of the visual world? It is possible to

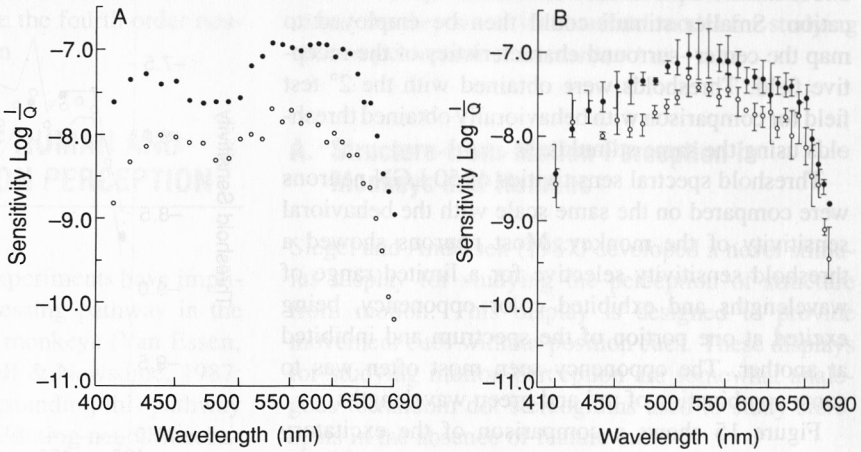

Fig. 13 (A) Photopic increment-threshold spectral sensitivity curves for a human observer taken at center fovea (filled) and at 14° away in the temporal retina (open). Note that there is a drop of about 1.0 log unit in sensitivity, with only minor differences in the shapes of the curves. (B) Photopic increment-threshold spectral sensitivity curves for a rhesus monkey taken under identical conditions as for (A). Note that the peak threshold sensitivity of the monkey is virtually identical to that of the human observer, and that the shape and drop in sensitivity with peripheral viewing are quite comparable to the human.

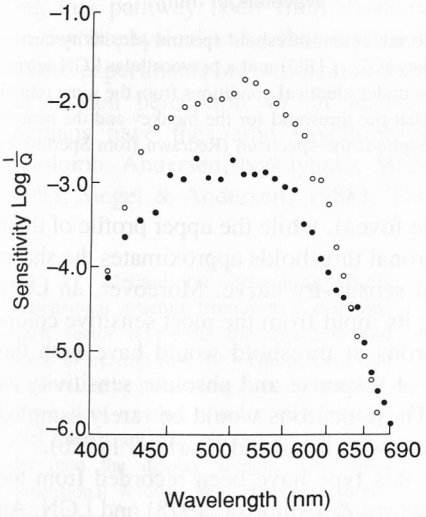

Fig. 14 Scotopic increment-threshold spectral sensitivity curves for a rhesus monkey for two retinal locations. Note that the rod-dominated sensitivity curve is about 1 log unit less sensitive in the fovea (filled) compared to that at 6° away in the temporal retina (open). This is comparable to changes seen in human observers (Crawford, 1977).

examine the visual brain directly using the combination of electrophysiological and behavioral techniques for insight as to how these mechanisms operate at the single-cell level to generate these behavioral functions.

B. Threshold Spectral Sensitivity of Monkey and Neurons

Rhesus monkeys were implanted with a stainless steel cylinder which accepted a head-mounted stereotaxic holder (Evarts, 1966). Varnished tungsten microelectrodes were then driven to the LGN of the alert behaving monkey by a micrometer-activated hydraulic system. Single neurons were isolated, and thresholds for monochromatic test flashes were measured for 22 wavelengths over the visible spectrum. Neurons were occasionally held for several hours, though responses (and thresholds) for single neurons were usually recorded for only a few minutes each. The tactic was to locate the receptive field for an LGN neuron and then, by shifting the fixation point, bring the perceptive field of the monkey into spatial registry so that both monkey and LGN neuron were "attending" to the same stimulus. The test stimulus was then reduced in intensity until the threshold was reached for the neuron and for the monkey (see Sperling et al., 1978).

The center of the receptive field of the LGN neuron was located by moving the fixation target in small steps and using a large 6° diameter test light, usually of 620 nm and high intensity. The experimenter rapidly covered the 18° field for a number of positions of the fixation target. The test light was then reduced to

2° for a finer determination of the receptive field location. Smaller stimuli could then be employed to map the center–surround characteristics of the receptive field. Thresholds were obtained with the 2° test field for comparison with behaviorally obtained thresholds using the same stimulus.

Threshold spectral sensitivities of 50 LGN neurons were compared on the same scale with the behavioral sensitivity of the monkey. Most neurons showed a threshold sensitivity selective for a limited range of wavelengths and exhibited color opponency, being excited at one portion of the spectrum and inhibited at another. The opponency seen most often was to some combination of red and green wavelengths.

Figure 15 shows a comparison of the excitatory component of several color-opponent units with the behaviorally measured threshold spectral sensitivity curve. It is clear that most of the peak sensitivities of the single units are less than the monkey's psychophysical sensitivity (all units had their receptive fields

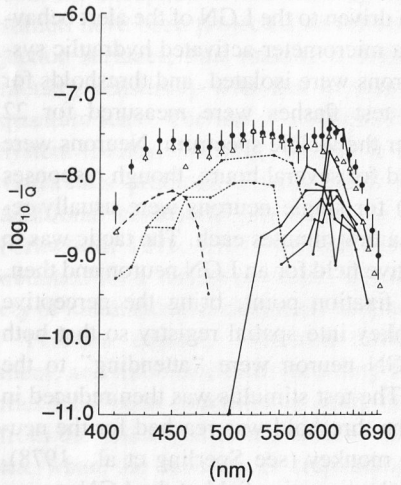

Fig. 15 Photopic increment-threshold spectral sensitivity curves for a 2° test flash at the center fovea (filled) and at 6° away (triangles). These curves are compared to the excitatory component of nine opponent-color neurons recorded from the parvocellular layers of the LGN. Note that the peak neuronal sensitivities are generally less than that of the psychophysical measures. The collective upper profile of these units approximates the shape, but not the sensitivity, of the behavioral curves.

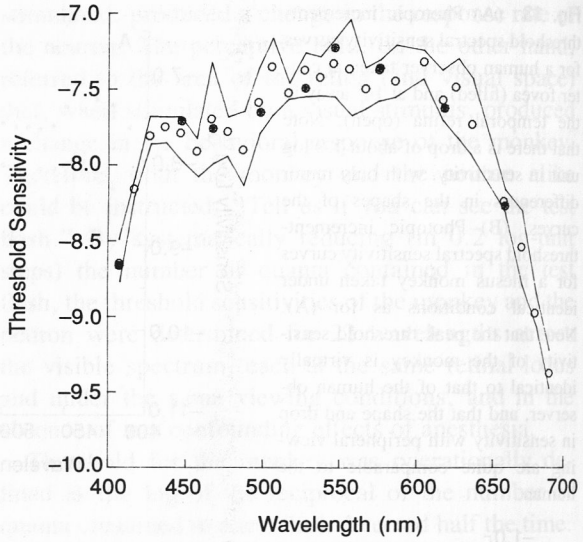

Fig. 16 Photopic increment-threshold spectral sensitivity curves for a rhesus monkey (○, ±1SD) and a parvocellular LGN broadband neuron taken under identical conditions from the same retinal locus (●). Note that the threshold for the monkey and the neuron are the same throughout the spectrum (Redrawn from Sperling et al., 1978).

within 6° of the fovea), while the upper profile of their collective neuronal thresholds approximates the shape of the spectral sensitivity curve. Moreover, an LGN neuron having its input from the most sensitive color-opponent neurons at threshold would have both the same breadth of response and absolute sensitivity as the monkey. These neurons would be rarely sampled since there are few at threshold (Barlow, 1972b).

Neurons of this type have been recorded from the pulvinar (Crawford & Espinoza, 1978) and LGN. An example of a parvocellular LGN unit appears in Fig. 16 (Sperling et al., 1978). This neuron had a broad spectral sensitivity which matched the behavioral threshold of the monkey. Thus, this neuron would be able to signal reliably whether a test flash had occurred.

These results show that at a very early stage in the primate visual system, single neurons display a threshold spectral sensitivity comparable to the behavioral response of the monkey. That is, in the response of a single neuron there is sufficient information to serve as the neural substrate for the monkey's

detection of a test light. This suggests that the gain of the visual system for photopic threshold detection must be determined at or before the fourth order neuron of the primate visual system.

VI. COMPARISON OF HUMAN AND MONKEY VISUAL MOTION PERCEPTION

Physiological and anatomical experiments have implicated a presumed motion processing pathway in the extrastriate cortex of macaque monkeys (Van Essen, 1985; Andersen, 1987; Maunsell & Newsome, 1987; Chapter 9, this volume). Understanding this pathway is an important first step in elucidating neural mechanisms for motion processing. One approach for studying this pathway is to train monkeys and humans in psychophysical tasks that test motion thresholds. These experiments have indicated that, for all aspects of motion perception so far tested, monkeys and humans have the same psychophysical thresholds (Golomb, Andersen, Nakayama, MacLeod & Wong, 1985; Siegel & Andersen, 1988). This suggests that the neural mechanisms underlying these percepts in the two species are the same, and it points to the macaque monkey as an ideal animal model for studying motion perception in humans.

A. Structure-from-Motion Perception in Monkeys and Humans

Siegel and Andersen (1987) developed a novel stimulus display for studying the perception of structure from motion. This display is designed to provide movement cues without position cues. These displays for studying motion perception are somewhat analogous to random dot stereograms used to study stereopsis in the absence of feature cues.

Figure 17 shows one of the displays used to study structure from motion. The display consists of randomly distributed moving dots that form the percept of a hollow, revolving cylinder. Each dot is present for a minimum period of time before being replotted at another random location on the surface of the cylinder. The minimum point life (exposure duration) serves several purposes, the most important being

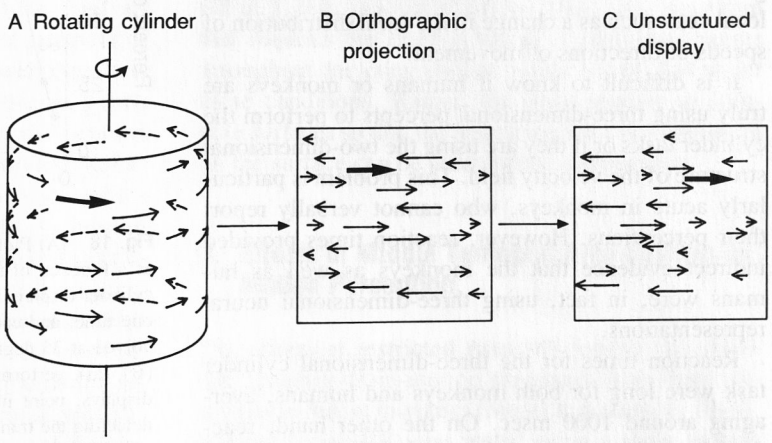

Fig. 17 Method for generating three-dimensional structure from motion displays. Each vector represents the direction and speed of moving dots. (A) The percept that is generated by the moving dot display is one of a hollow, rotating cylinder. (B) The parallel (orthographic) projection of the cylinder onto the display screen. This two-dimensional velocity field gives rise to the three-dimensional percept in A. (C) The unstructured display that is computed by displacing each point by a random amount up to the limit of the entire width of the display. The fate of an individual trajectory is shown by the bold arrow. The point density on the surface of the display is kept constant by displaying each moving dot for a finite amount of time. New dots appear at random locations on the display and follow new trajectories. From Siegel and Andersen (1988). Reprinted by permission from *Nature*, **331**, pp. 259–261. Copyright © 1987 Macmillan Journals Limited.

the removal of position cues when the display goes through a transition from no structure to structure.

The subjects perform a reaction time task in which they must detect the transition from an unstructured noise pattern to the revolving cylinder. The noise pattern has all the same vectors as the structured stimulus, the only difference being that the vectors are randomly shuffled, thus destroying the structure. If the transition is made to a display that is only partially structured, often the cylinder can still be perceived, but with more difficulty. For example, a cylinder with a fraction of structure of 0.5 has each of its points perturbed by a random amount up to a limit of 0.5 of the diameter of the display. By varying the fraction of structure in the test stimulus, psychometric functions can be generated.

Figure 18 shows psychometric functions for one monkey and one human performing the three-dimensional cylinder task. The curves in each panel are similar, indicating that the two species have similar abilities to detect structure from motion in the three-dimensional display. Monkeys and humans also had similar thresholds for the two-dimensional structures of rigid rotation and nonrigid expansion. Control experiments indicated that the subjects were using the global structure of the display to do the task and not local cues such as a change in the local distribution of speeds or directions of movement.

It is difficult to know if humans or monkeys are truly using three-dimensional percepts to perform the cylinder tasks or if they are using the two-dimensional structure of the velocity field. This problem is particularly acute in monkeys, who cannot verbally report their perceptions. However, reaction times provided indirect evidence that the monkeys as well as humans were, in fact, using three-dimensional neural representations.

Reaction times for the three-dimensional cylinder task were long for both monkeys and humans, averaging around 1000 msec. On the other hand, reaction times for the two-dimensional tasks of rotation and expansion were considerably shorter, averaging around 600 msec. A difference of 400 msec in terms of neural computation time is quite significant. If one examines the two-dimensional cues available in the

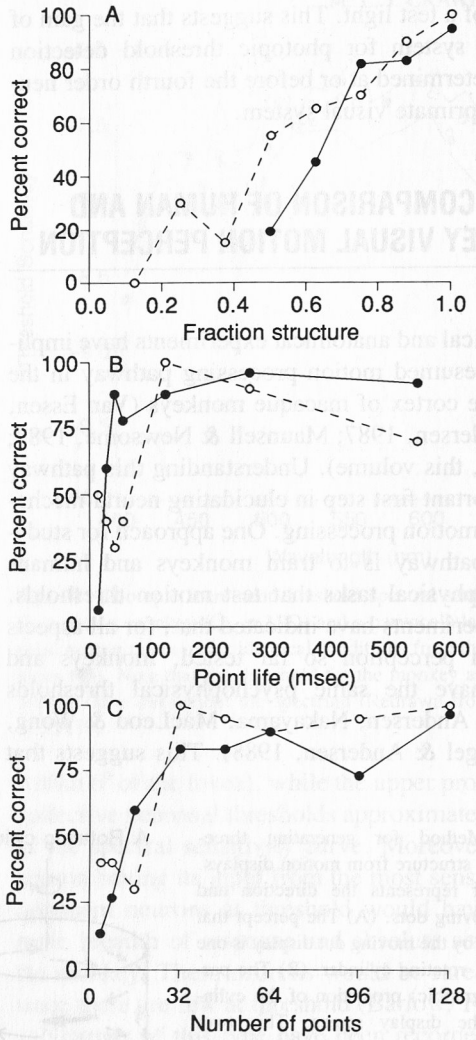

Fig. 18 (A) Plot of performance of one monkey and one human as a function of the fraction of structure in the three-dimensional cylinder display. In this experiment 128 points were visible at any one time, and each point was on for 532 msec. The cylinder revolved at 35 degrees/sec, and the screen refresh rate was 35 Hz. (B) Task performance as a function of point life. For 128 point displays, point lives of under 100 msec reduced performance in detecting the transition from noise to a three-dimensional cylinder of 0.875 fraction structure. Refresh rate was 70 Hz, and the angular velocity was 35 degrees/sec. (C) Task performance as a function of the number of dots. The same parameters as in B were used, but the point life was held constant (532 msec) and the number of points varied. Performance deteriorated below 32 points. From Siegel and Andersen (1988). Reprinted by permission from *Nature*, **331**, 259–261. Copyright © 1987 Macmillan Journals Limited.

three-dimensional cylinder and two-dimensional rotation tasks, those cues are found to be very similar; the cylinder has fast speeds in the center of the display and slow speeds in the surround, whereas the rotation has slow speeds in the center and fast speeds in the surround. Thus one would assume that if the subjects were using only two-dimensional cues available in the velocity field, then the reaction times should be more similar. The increased reaction time could not be accounted for by the fact that the cylinder was hollow and required the segregation of two surfaces, whereas the two-dimensional rotation had only one surface. In tasks where two two-dimensional rotations in opposite directions were used, the reaction time increased at most by 50 msec. In conclusion, these experiments suggest that monkeys (and humans) use three-dimensional neural representations to perform these tasks.

B. Characteristics of Spatio-Temporal Integration

Having developed the three-dimensional structure-from-motion task, it was possible to ask how motion information is integrated in space and time to form the three-dimensional percepts. This issue had already been approached from a theoretical perspective by Ullman (1979), who showed that "given three distinct orthographic views of four non-coplanar points in a rigid configuration, the structure and motion compatible with the three views are uniquely determined." Obviously, 4 points and 3 frames are only a theoretical limit, and the brain is likely to require more points and time since there is much noise in neural signals. Also, the brain is likely to use an algorithm for retrieving structure from motion that does not perform at the theoretical optimum. To examine temporal integration, the exposure duration of the individual points was changed, and the spatial integration was studied by changing the number of points.

Figure 18B shows that in both monkeys and humans performance in the three-dimensional cylinder task is reduced when the lifetime falls below 100 msec for 128 points. Figure 18C indicates that both species do poorly when there are less than 32 points with point lives of 500 msec. Moreover, a trade-off between point life and point number was found with shorter point lives requiring more points and vice versa.

C. Structure-from-Motion Computation Involves Formation of Three-Dimensional Surface Representations

There are three elements in the above experiments suggesting that three-dimensional percepts of surfaces result from integration of information from the velocity field. The first bit of evidence derives from masking experiments and shows that information is used from the entire surface for performing the task. The second kind of evidence concerns the reaction time data and indicates that the computation time varies with the type of surface being computed. Yet, the most compelling evidence for surface representations comes from the third piece of evidence, the time integration experiments. Recall from the reaction time data that it requires 1000 msec to perform the three-dimensional surface task. However, the individual points are visible for only 100 msec before being plotted at a new, random location. Thus, any algorithm that requires the exact position of individual points throughout the computation period would fail under these conditions. Rather, the brain appears to compute surfaces so that the appearance of a dot anywhere on the surface can be used for the computation.

D. Effects of Middle Temporal Area Lesions on Motion Perception

The effects of restricted Area MT lesions on motion and structure-from-motion thresholds have been examined in rhesus monkeys (Siegel & Andersen, 1986). Motion thresholds were tested using a shear motion detection task. This was a reaction time task in which the animal had to release a lever with the onset of a shear motion stimulus in a previously static random dot display (Golomb et al., 1985). The structure-from-motion task was the three-dimensional cylin-

der task described previously. Psychometric functions were generated by varying the amplitude of the shear motion.

Prior to the lesions, motion thresholds were determined at different retinal locations. In this procedure the animal fixated a small point at the start of each trial, and the test stimuli were then presented at different locations in the visual field. Next, the retinotopic representation in Area MT was mapped using microelectrodes. Area MT contains a representation of the contralateral visual field that results from the systematic anatomical mapping of the retinas via the lateral geniculate nucleus and earlier visual cortical Areas V1 and V2. A small lesion was made at a selected location in this retinotopic map using the neurotoxin ibotenic acid. Motion thresholds were then retested to measure the effects of these lesions on motion perception.

The use of ibotenic acid is an important control. This compound destroys cell bodies but not fibers of passage. This selectivity is important because the optic radiation (the projection from the lateral geniculate nucleus to primary visual cortex) passes directly below Area MT. A surgical ablation of Area MT would likely also damage these fibers, producing a nonspecific lesion. The nonspecificity of the lesion would complicate the interpretation of lesion induced deficits.

Figure 19 shows the results of an MT lesion made in the lower visual field contralateral to the side of the lesion. Shear motion thresholds show a dramatic increase confined largely to the area of the visual field that corresponds to the retinotopic locus of the lesions. An important observation is that this deficit recovered in 3 to 4 days. Control experiments showed that contrast thresholds were not affected by these lesions. Thus, the increased motion thresholds were not due to the animal's being blind at the locus of the lesion. Rather, the deficit was selective for motion perception.

Another experiment tested the effect of Area MT lesions on three-dimensional structure-from-motion perception. The animal was not able to perceive the cylinder even at 100% structure. Again the deficit was restricted to the area of the visual field that corresponded to the retinotopic locus of the lesion. Interestingly the deficit remained long after the shear thresholds had recovered and was still prominent at 23 days post lesion.

E. Summary of Motion Experiments

The psychophysical experiments indicate that monkeys and humans have similar abilities to detect structure from motion. Several lines of evidence further suggest that in our three-dimensional tasks the brain is forming representations of surfaces by integrating information from the velocity field over space and time.

Lesion experiments indicate that Area MT is important for perceiving motion and structure from motion. However, there is rapid recovery in motion deficits following the lesions, suggesting that the brain undergoes a functional reorganization. There are two possible mechanisms for this recovery: (1) reorganization within Area MT and (2) reorganization of parallel pathways around Area MT. Experiments that totally ablate Area MT can distinguish between these two possibilities. Another question is the role of training and visual experience on recovery. Would visual deprivation prevent recovery? These and many other interesting experiments examining plasticity in adult brain are made possible because the connectivity, and increasingly the function, of the visual extrastriate cortex is becoming better understood.

VII. CONCLUSIONS

These contributions demonstrate the enormous value in the use of research animals to model physiological processes thought to underlie sensory and perceptual processes in humans. These are only examples of animal research on topics which are covered in more detail in subsequent chapters.

Relative to the linking propositions, and their atten-

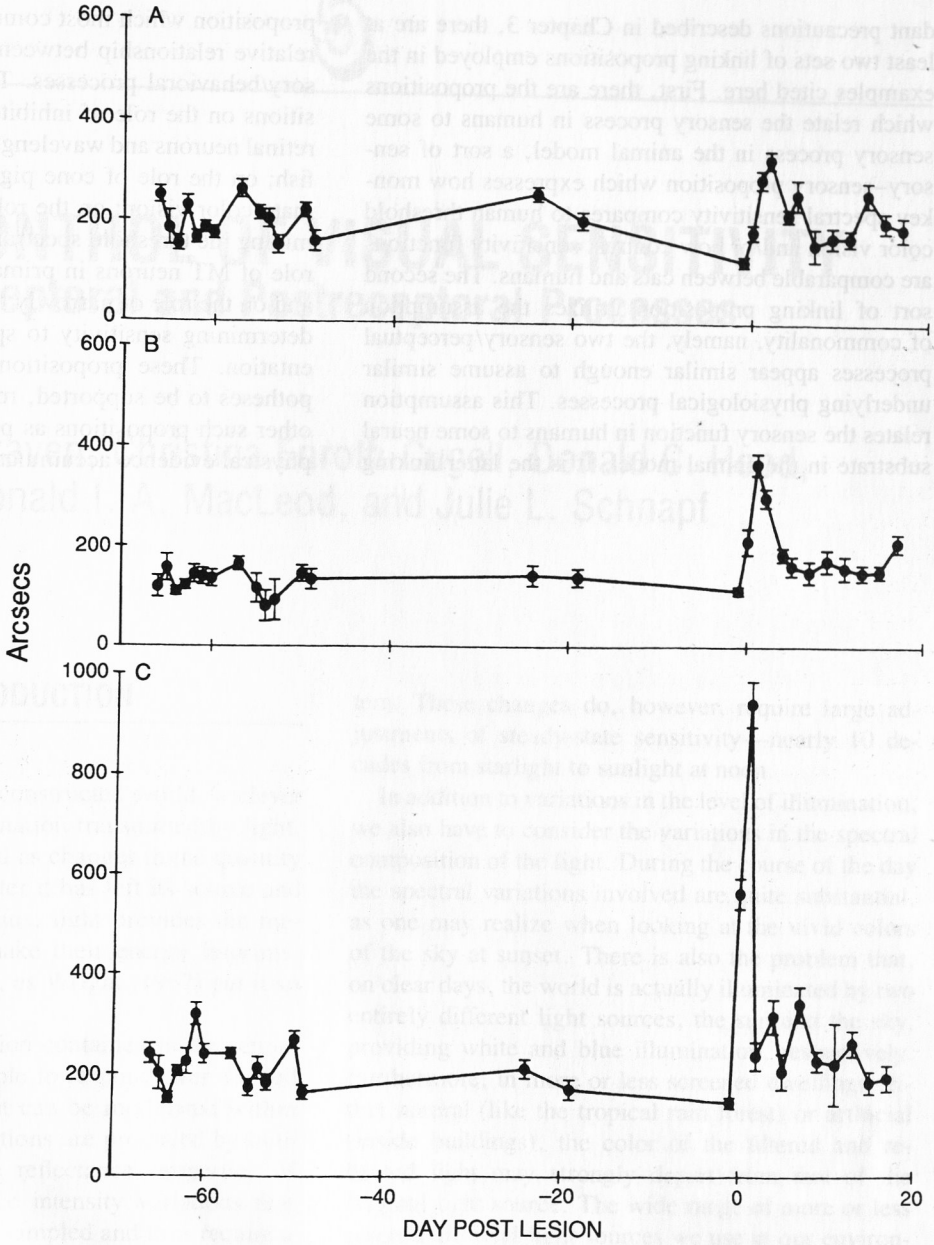

Fig. 19 The effect of ibotenic acid lesions in visual Area MT on shear motion thresholds of the monkey for three visual field locations. Fifty percent hit rates are plotted from psychometric curves in which spatial and temporal frequency is held constant and amplitude is varied. The lesion was placed in the lower visual field representation of Area MT in the contralateral (right) hemisphere. Little effect is seen for central and upper field locations (top and middle), and the greatest effect is focused at the lower field location (bottom) with thresholds increasing after 1 day to over 900 arc sec. Also note that the thresholds recover rapidly in a few days.

dant precautions described in Chapter 3, there are at least two sets of linking propositions employed in the examples cited here. First, there are the propositions which relate the sensory process in humans to some sensory process in the animal model, a sort of sensory–sensory proposition which expresses how monkey spectral sensitivity compares to human threshold color vision and/or how contrast sensitivity functions are comparable between cats and humans. The second sort of linking proposition utilizes the assumption of commonality, namely, the two sensory/perceptual processes appear similar enough to assume similar underlying physiological processes. This assumption relates the sensory function in humans to some neural substrate in the animal model. It is the latter linking proposition which most commonly expresses the correlative relationship between brain function and sensory/behavioral processes. These are explicit propositions on the role of inhibitory interactions between retinal neurons and wavelength discrimination in goldfish; on the role of cone pigments in anomalous primate color vision; on the role of LGN cells in determining the threshold spectral sensitivity curve; on the role of MT neurons in primate sensitivity to motion; and on the role of narrowly tuned cat cortical neurons determining sensitivity to spatial frequency and orientation. These propositions stand as working hypotheses to be supported, rejected, or supplanted by other such propositions as physiological and psychophysical evidence accumulates.